(4)

REPAIR, EVALUATION, MAINTENANCE, AND REHABILITATION RESEARCH PROGRAM

TECHNICAL REPORT REMR-CS-15

ANALYSIS OF CONCRETE CRACKING IN LOCK WALL RESURFACING

by

C. Dean Norman, Roy L. Campbell, Sr., Sharon Garner

•Structures Laboratory

DEPARTMENT OF THE ARMY
Waterways Experiment Station, Corps of Engineers
PO Box 631, Vicksburg, Mississippi 39180-0631

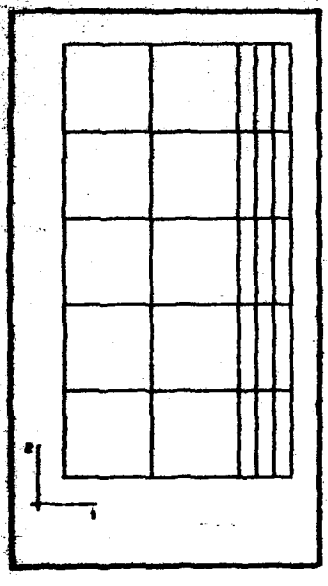

August 1988
Final Report

Prepared for DEPARTMENT OF THE ARMY
US Army Corps of Engineers
Washington, DC 20314-1000
Under Civil Works Research Work Unit 32273

The following two letters used as part of the number designating technical reports of research published under the Repair, Evaluation, Maintenance, and Rehabilitation (REMR) Research Program identify the problem area under which the report was prepared:

	Problem Area		Problem Area
CS	Concrete and Steel Structures	EM	Electrical and Mechanical
GT	Geotechnical	EI	Environmental Impacts
HY	Hydraulics	OM	Operations Management
CO	Coastal		

Destroy this report when no longer needed. Do not return it to the originator.

The findings in this report are not to be construed as an official Department of the Army position unless so designated by other authorized documents.

The contents of this report are not to be used for advertising, publication, or promotional purposes. Citation of trade names does not constitute an official endorsement or approval of the use of such commercial products.

COVER PHOTOS:

TOP — Cracking in lock wall resurfacing

BOTTOM — Typical lock-wall finite element grid

Unclassified
SECURITY CLASSIFICATION OF THIS PAGE

REPORT DOCUMENTATION PAGE

Form Approved
OMB No 0704 0188
Exp Date Jun 30 1986

1a REPORT SECURITY CLASSIFICATION Unclassified	1b RESTRICTIVE MARKINGS
2a SECURITY CLASSIFICATION AUTHORITY	3 DISTRIBUTION/AVAILABILITY OF REPORT Approved for public release; distribution unlimited
2b DECLASSIFICATION/DOWNGRADING SCHEDULE	
4 PERFORMING ORGANIZATION REPORT NUMBER(S) Technical Report REMR-CS-15	5 MONITORING ORGANIZATION REPORT NUMBER(S)
6a NAME OF PERFORMING ORGANIZATION USAEWES Structures Laboratory 6b OFFICE SYMBOL (If applicable) WESSC	7a NAME OF MONITORING ORGANIZATION
6c ADDRESS (City, State, and ZIP Code) PO Box 631 Vicksburg, MS 39180-0631	7b ADDRESS (City, State, and ZIP Code)
8a NAME OF FUNDING/SPONSORING ORGANIZATION US Army Corps of Engineers 8b OFFICE SYMBOL (If applicable)	9 PROCUREMENT INSTRUMENT IDENTIFICATION NUMBER
8c ADDRESS (City, State, and ZIP Code) Washington, DC 20314-1000	10 SOURCE OF FUNDING NUMBERS PROGRAM ELEMENT NO / PROJECT NO / TASK NO / WORK UNIT ACCESSION NO 32273

11 TITLE (Include Security Classification)
Analysis of Concrete Cracking in Lock Wall Resurfacing

12 PERSONAL AUTHOR(S)
Norman, C. Dean; Campbell, Roy L., Sr.; Garner, Sharon

13a TYPE OF REPORT	13b TIME COVERED	14 DATE OF REPORT (Year, Month, Day)	15 PAGE COUNT
Final Report	FROM _____ TO _____	August 1988	53

16 SUPPLEMENTARY NOTATION This is a report of the Concrete and Steel Structures problem area of the Repair, Evaluation, Maintenance, and Rehabilitation (REMR) Research Program. Available from National Technical Information Service, 5285 Port Royal Road, Springfield, VA 22151.

17 COSATI CODES			18 SUBJECT TERMS (Continue on reverse if necessary and identify by block number)
FIELD	GROUP	SUB-GROUP	Aging, Concrete constitutive model, Creep, Lock walls, Overlays, Shrinkage, Thermal effects

19 ABSTRACT (Continue on reverse if necessary and identify by block number)

An aging constitutive model for concrete including creep, shrinkage, and cracking is used in a general-purpose heat transfer and structural analysis finite element code to predict the response of concrete overlays placed on lock wall surfaces. Model predictions corresponded well with test results. The model was used to predict the response of concrete overlays with varying thicknesses and placement conditions. In all of the analyses, shrinkage had a dominant effect on cracking. Ambient temperature, thickness of overlay, and use of a bond breaker also significantly affected cracking. Recommendations include careful curing procedures and the use of mix proportions that minimize shrinkage and emphasize the importance of early-time materials property tests in predicting stresses and cracking.

20 DISTRIBUTION/AVAILABILITY OF ABSTRACT	21 ABSTRACT SECURITY CLASSIFICATION
☒ UNCLASSIFIED/UNLIMITED ☐ SAME AS RPT ☐ DTIC USERS	Unclassified
22a NAME OF RESPONSIBLE INDIVIDUAL	22b TELEPHONE (Include Area Code) / 22c OFFICE SYMBOL

DD FORM 1473, 84 MAR 83 APR edition may be used until exhausted
All other editions are obsolete

Unclassified

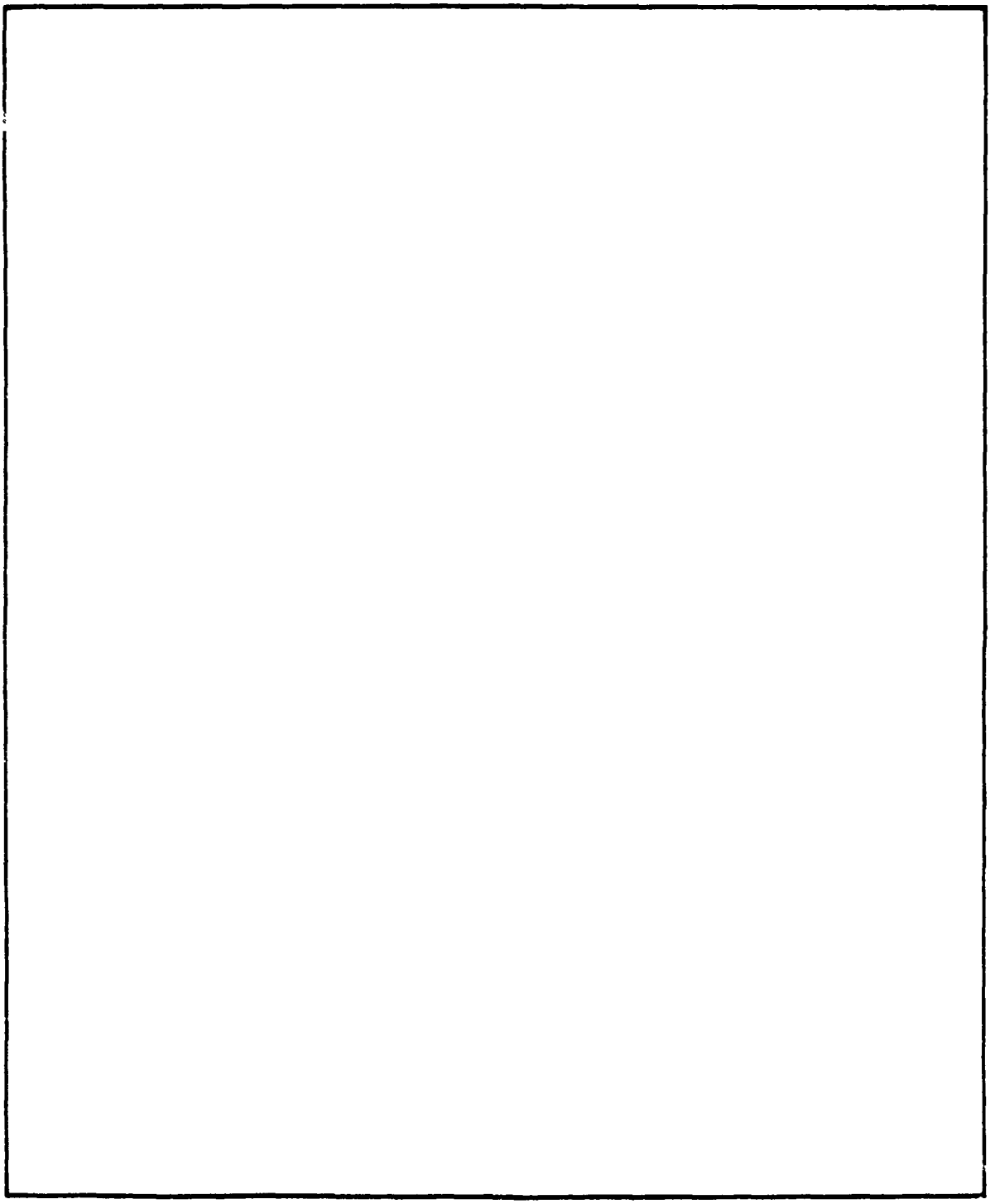

PREFACE

The investigation described in this report was conducted by the Concrete Technology Division (CTD), Structures Laboratory (SL), US Army Engineer Waterways Experiment Station (WES). Publication of the report was funded under Civil Works Research Work Unit 32273, "Rehabilitation of Navigation Locks," for which Mr. James E. McDonald is Principal Investigator. This work unit is part of the Concrete and Steel Structures Problem Area of the Repair, Evaluation, Maintenance, and Rehabilitation (REMR) Research Program sponsored by Headquarters, US Army Corps of Engineers (HQUSACE). The Overview Committee of HQUSACE for the REMR Research Program consists of Mr. James E. Crews and Dr. Tony C. Liu. Technical Monitor for this study is Dr. Liu.

The investigation was performed under the general supervision of Mr. Bryant Mather, Chief, SL, and Mr. Kenneth Saucier, Chief, CTD. Program Manager for REMR is Mr. William F. McCleese, CTD. This report was prepared by Messrs. C. Dean Norman and Roy L. Campbell, Sr., and Mrs. Sharon B. Garner. Final editing and figure and text layout were coordinated by Mrs. Gilda Miller, editor, and Mrs. Chris Habeeb, editorial assistant, Information Products Division, Information Technology Laboratory, WES. Permission to reproduce copyrighted material was granted by the American Concrete Institute.

COL Dwayne G. Lee, CE, is the Commander and Director of WES, and Dr. Robert W. Whalin is Technical Director.

CONTENTS

CONVERSION FACTORS, NON-SI TO SI (METRIC) UNITS OF MEASUREMENT

Non-SI units of measurement used in this report can be converted to SI (metric) units as follows:

Multiply	By	To Obtain
Fahrenheit degrees	5/9	Celsius degrees or kelvins*
feet	0.3048	metres
inches	25.4	millimetres
pounds (force) per square inch	0.006894757	megapascals
pounds (mass)	0.4535924	kilograms
pounds (mass) per cubic foot	16.01846	kilograms per cubic metre

* To obtain Celsius (C) temperature readings from Fahrenheit (F) readings, use the following formula: $C = (5/9)(F - 32)$. To obtain kelvin (K) readings, use: $K = (5/9)(F - 32) + 273.15$.

ANALYSIS OF CONCRETE CRACKING IN LOCK WALL RESURFACING

PART I: INTRODUCTION

Background

1. More than half of the 260 lock chambers maintained by the US Army Corps of Engineers are more than 40 years old. Many of these older structures are currently in need of extensive rehabilitation; others will require repair and rehabilitation in the near future. Since renovation of a single navigation lock typically costs between $10 million and $30 million, there is a need for evaluation and development of materials and repair techniques to ensure optimum utilization of available resources. A significant problem encountered in lock wall repair has been cracking in the replacement concrete. This problem has occurred on all lock rehabilitation projects to date. An example of typical cracking is shown in Figure 1 for Lock and Dam No. 1 (L&D No. 1) on the Mississippi River. At L&D No. 1, cracking (observed as early as 1 day after placement) generally extended completely through the 12- to 18-in.-thick replacement slab. The use of expansive cement and the inclusion of control joints has been of some help, although the problem has not been eliminated. These corrective efforts predominately have been of a trial-and-error nature and can be assessed only on a case-by-case basis. A rational and consistent assessment of the cracking problem can be developed best by evaluating the effects on crack initiation of such parameters as early-age mechanical and thermal properties of concrete, concrete placement temperatures, form insulation, thickness of overlay, reinforcing steel, bond breaker along interface, form removal time, etc. Currently, well established heat transfer and structural analysis finite element codes exist which provide precise and efficient numerical formulations for simulating the curing of the lock wall resurfacing slab. However, there are unique problems associated with cracking in the resurfacing slab. Since cracks have been observed as early as 1 day after placement, the numerical analysis must be based on material properties such as modulus, tensile strain capacity, creep, shrinkage, etc., which are determined at times as early as 1 day in addition to traditional later-time values. Very limited early-time material properties data are available and, in general,

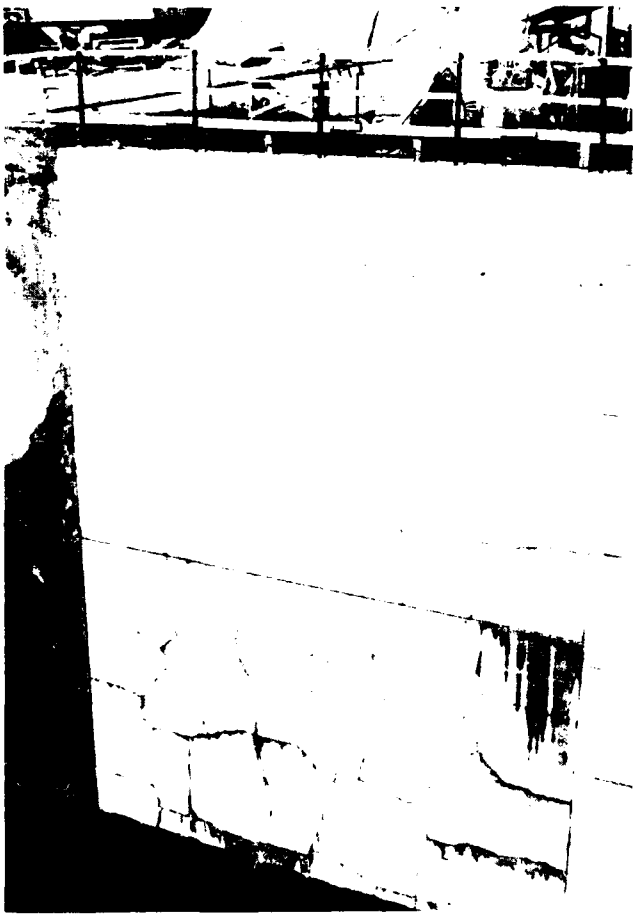

Figure 1. Cracking in lock wall resurfacing

a greater uncertainty is associated with it than the more abundant later-time data. Other problems which present special difficulty are accurate specification of the mechanical and thermal boundary conditions along the line of contact between the fresh concrete and the formwork. The formwork provides a force resisting the thermal expansion of the new concrete and a resistance to heat transfer across the boundary. Neither of these boundary conditions is precisely known. The parameter of greatest uncertainty along the line of contact between the fresh concrete and the old concrete is the friction or bond between the two concretes. To determine quantitative descriptions, all boundary conditions affecting the problem and early-time material properties would require extensive laboratory and field tests. Another approach to the problem is to use limited material properties test data along with different boundary condition assumptions which are felt to bound the actual field values. These material properties and boundary conditions can then be incorporated in an efficient finite element code and a parameter study can be made to determine repair, design, and construction procedures which minimize the potential for cracking. The latter approach will be discussed in detail in this report.

Objectives

2. The general objective of this study is to develop new and improved materials and design/construction techniques for use in navigation lock rehabilitation. The specific objectives of this study are to determine and evaluate parameters which significantly affect cracking in resurfacing slabs.

Scope

3. This study uses a modern general-purpose heat transfer and structural analysis finite element (FE) code for the numerical formulation of a typical lock wall resurfacing slab problem. Several thermal stress analyses are performed using varying parameters to evaluate the effects on producing or inhibiting cracking in the resurfacing slab. Based on results of the parameter study, the most desirable values for key parameters are recommended.

PART II: ANALYSIS PROCEDURE

Heat Transfer and Structural Analysis

4. As mentioned previously, a well established general-purpose finite element code was selected for use in analyzing and evaluating the lock wall resurfacing problem. ABAQUS, developed by Hibbitt, Karlsson, and Sorensen,* was the finite element code selected for this problem based on its flexibility, and demonstrated effectiveness in other similar ongoing analysis projects at the US Army Engineer Waterways Experiment Station (WES). The theoretical formulation of ABAQUS relies on the finite element stiffness method with some hybrid formulations included as necessary. The code includes both user and automatic control of solution step size. Input is in free format, key worded, and makes use of set definitions for easy cross reference. A broad element library is included in ABAQUS, and any combination of elements can be used in the same model. A wide variety of constitutive models is also provided in ABAQUS, and these models can be used essentially with any element type. User-defined material models are incorporated with relative ease through the UMAT subroutine. Also, reinforcement (rebar) can be added to any element. Static and dynamic response in stress analysis can be conducted as well as steady-state and transient heat transfer problems. Incremental construction problems can be simulated effectively through the "model change" option where previously defined elements can be included or removed from the analysis in a specified solution step. Specific details of element type and boundary conditions used will be presented in the various analysis phases of this report.

Aging Creep Model with Cracking

5. The fact that the material properties of concrete change with time (aging) presents special computational problems for the thermal stress analysis of the lock wall resurfacing slab. Significant changes in material

---

* Hibbitt, Karlsson, and Sorensen, Inc. 1983. ABAQUS User's Manual, Providence, R.I.

strength, modulus, creep, shrinkage, etc. must be accounted for in a consistent and numerically efficient manner in the finite element solution procedure. This was accomplished by developing a two-dimensional (2-D) aging creep model with cracking capabilities in the ABAQUS-UMAT subroutine format. In this model, cracking the xy (or rz) plane and normal to the θ direction for axisymmetric problems is included. The model also includes the effects of aging on the elastic modulus and cracking strength and the effects of changing temperatures on the creep compliance, the elastic modulus, and the ultimate/cracking strength. The elastic modulus and ultimate strength can be expressed as functions of age (t) and temperature (T) as $E(t,T)$ and $\sigma_u(t,T)$, respectively. The cracking strain (ε_f), if not user defined, is assumed to be 10 percent of the absolute value of the compressive strain at ultimate strength. Poisson's ratio (ν) is assumed to be constant. The creep properties, Equation 1 and the properties $E(t,T)$, $\sigma_u(t,T)$, ε_f, and ν are included in a separate subroutine in a form which can be easily modified by the user. The numerical values of the model parameters, namely those describing Equation 1, and the other mechanical properties are supplied by the user. Further details of the mathematical description of the model are presented by Rashid and Dunham.* Creep properties are given in the form

$$J(t,\tau,T) = \sum_{i=1}^{2} A_i(\tau,T)\left[1 - e^{-r_i(t-\tau)}\right] + D(\tau,T)(t - \tau) \qquad (1)$$

$$A_i(\tau,T) = A_{0i}\, e^{-Q/RT}\left[\frac{E(3)}{E(\tau)}\right]^2$$

$$D(\tau,T) = D_0\, e^{-Q/RT}\left[\frac{E(3)}{E(\tau)}\right]^2$$

where

J = creep strain per unit stress

t = time

τ = age at loading

T = temperature

---

* Y. R. Rashid and R. S. Dunham. "Development of a General Three-Dimensional UMAT Model for Concrete Considering Aging, Viscoplasticity, and Cracking," Technical Report ANA-85-0041, (in preparation), ANATECH International Corp., La Jolla, CA.

R = gas constant

$E(\tau)$ = modulus of elasticity at time τ

r_i, A_i, D, Q = material constants

6. The material constants are calibrated so that J best represents the specific creep of a particular concrete during a specified time frame of interest. For example, to develop the specific creep function based on an age at loading of 3 days, one selects an experimental curve with the desired characteristics. Three times are determined for accurate curve fits (e.g., $(t - \tau)$ = 1 day, 7 days, and 28 days). Parameters r_1 and r_2 are determined so that the terms $e^{r_i(t-\tau)}$ saturate at $(t - \tau) = 1$ and 28 (i.e., $e^{-r_1(4-3)} = e^{-r_2(31-3)} = 0.005$, or smaller). With $\tau = 3$, r_1 and r_2 known $J(t_i, 3)$ at the three times of interest are measured from the creep curves and substituted in the three equations

$$J(t_i, 3) = A_1 \left[1 - e^{-r_1(t_i-3)}\right] + A_2 \left[1 - e^{-r_2(t_i-3)}\right] + D(t_i - 3) \qquad (2)$$

where

$$i = 1, 2, 3$$

to determine A_1, A_2, and D. The linear term $D(t - \tau)$ can be replaced with another exponential term if necessary. The effect of aging is accounted for in the term $E(3)/E(\tau)$ and will be discussed later. Temperature effects are simulated through the activation energy term $e^{-Q/RT}$, where Q is best evaluated through creep tests at different temperatures, in which $J(t, \tau,$ and $Ti)$ can be measured and set equal to $e^{-Q/RTi}$ for the two values of Ti at fixed t and τ. The equation below can then be solved for Q

$$\frac{e^{-Q/RT_1}}{e^{-Q/RT_0}} = \frac{J(t, \tau, T_1)}{J(t, \tau, T_0)}$$

If creep tests at several temperatures are available, Q can be determined as a function of temperature.

7. Similar approaches are used to determine the elastic modulus as a function of time and shrinkage as a function of time. The functional form for $E(\tau)$, where τ is concrete age in days, is

$$E(\tau) = E_0 + B_1\left[1 - e^{-m_1(\tau-1)}\right] + B_2\left[1 - e^{-m_2(\tau-1)}\right] + B_3(\tau-1)$$

where E_0 is one-day modulus and constants B_1, B_2, and B_3 are determined based on tests at 3 days of interest. Shrinkage is determined from

$$\varepsilon^s = C_1(1 - e^{-s_1 t}) + C_2(1 - e^{-s_2 t})$$

where S_1 and S_2 are selected as in the previous forms so that shrinkage becomes negligible after some time. Then C_1 and C_2 are determined from early-time and late-time sealed shrinkage tests. These tests primarily measure autogenous shrinkage (shrinkage that occurs without a loss of moisture). Most shrinkage that occurs in mass concrete structures is of this type, since only the exterior faces are subject to drying.

8. Cracking is assumed to occur when a cracking criterion is satisfied. This criterion consists of the following elements: (a) it is strain driven but is modified by the stress, as will be shown later; (b) the crack surface normal is in the direction of the principal strain; and (c) the cracking criterion is interactive. This criterion is implemented as follows. Consider a trace of the 2-D failure surface shown in Figure 2 in principal stress space. The f'_t and f'_c have the usual meaning, namely tensile and compressive strengths, respectively. For isotropic material, which describes concrete prior to cracking, the principal strain and principal stress directions coincide. Therefore, one could also express the cracking criterion in terms of the principal strains. It is important to do so for concrete if we are to predict cracking correctly. Consider, for example, a cube of material pressure loaded with σ_2. The cube will split in the direction of the load, under the effect of the ε_1 strain. The σ_1 stress will be a small positive, actually zero in a finite element plane stress analysis. If the cracking criterion is a function of the stress only, then from Figure 2 cracking occurs only when σ_2 approaches the ultimate uniaxial compressive strength. The ε_1 strain is $-\nu\,\varepsilon_2 = -\nu(\sigma_2/E)$. If $\sigma_2 = f'_c$, then the cracking strain is calculated to be 20 percent of the uniaxial ultimate compressive strain, or twice the value usually assumed. One concludes from this example that a strain-dependent cracking criterion is more appropriate. Now let us consider the same example, but with sufficiently small σ_2 so that immediate cracking does not occur. If σ_2 is sustained for a long enough time, cracking could

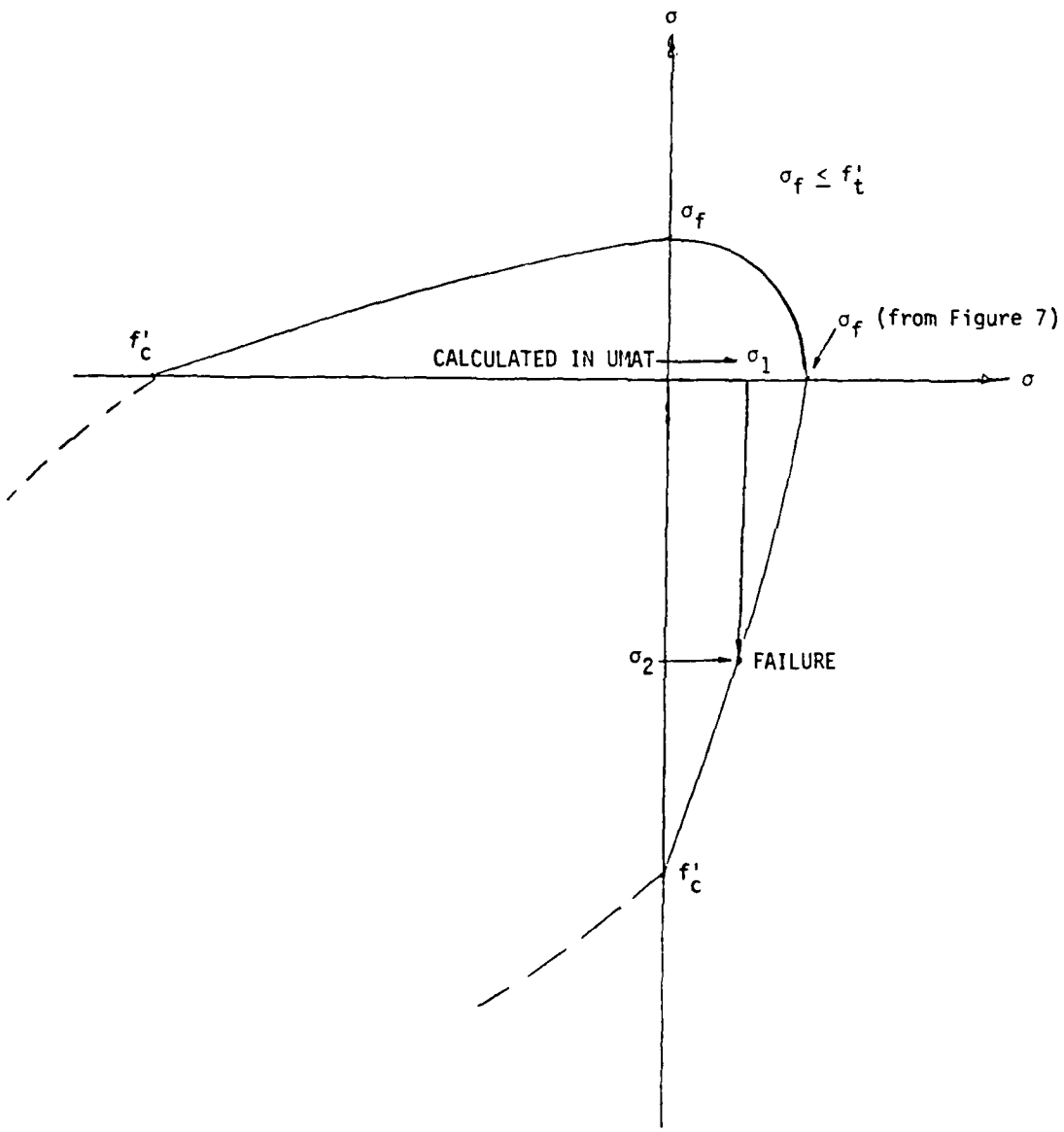

Figure 2. Concrete fracture surface

eventually occur as a result of the added creep strain ε_1^c. The total cross strain becomes $\varepsilon_1 = -\nu(\sigma_2/E) + \varepsilon_1^c$. The material shows higher tensile strain capacity under creep, and it may be concluded from this that the cracking criterion should be time-dependent. A stress-alone or strain-alone cracking criterion will not be general enough for a time-dependent analysis, and there is a lack of time-dependent cracking data. Therefore, to accommodate the creep and relaxation effects together with elastic stress and strain states without new experiments, an interactive criterion must be adopted. This is illustrated in Figure 3 which describes a linear relationship between the cracking stress and the cracking strain. The uniaxial tension test is the midpoint of the straight line that crosses the ε and σ axes at $2f_t'/E$ and $2f_t'$, respectively. Several familiar test conditions are indicated in the figure. The actual interaction curve is indicated by the broken line. Note that cracking under zero strain is physically impossible for compressible materials (with Poisson's ratio < 0.5). The shape of the curve in Figure 3 is obviously data dependent, but for simplicity, it is assumed to be a straight line. The factor of 2 is arbitrary. It is used to expand the curve above and below the midpoint to accommodate cracking at high stress (low strain) and low or zero stress (high strain), as well as creep-induced cracking. Although creep-cracking data are scarce, there is some evidence that creep-cracking strain is approximately twice that of the uniaxial tensile strength. Implementation of this criterion in the model is as follows:

a. Calculate the maximum principal strain ε_1 in UMAT.

b. Enter Figure 3 with ε_1 and calculate σ_f.

c. Adjust the failure surface (Figure 2) amplitude, using σ_f as the intercept, instead of f_t'.

d. Enter Figure 2 using the principal stresses σ_1 and σ_2 calculated in UMAT, and calculate whether the (σ_1, σ_2) point penetrates the failure surface. If so, introduce a crack with normal in the principal strain direction and formulate the constitutive matrix in the principal coordinate system.

e. Rotate the precracking stresses to the principal coordinate system and adjust these stresses to reflect the new cracking state.

f. Rotate the constitutive matrix and the stresses back to the coordinate system of the structure.

g. The new constitutive matrix and stresses are then used by ABAQUS to calculate the nodal forces and the tangent stiffness matrix in the next step.

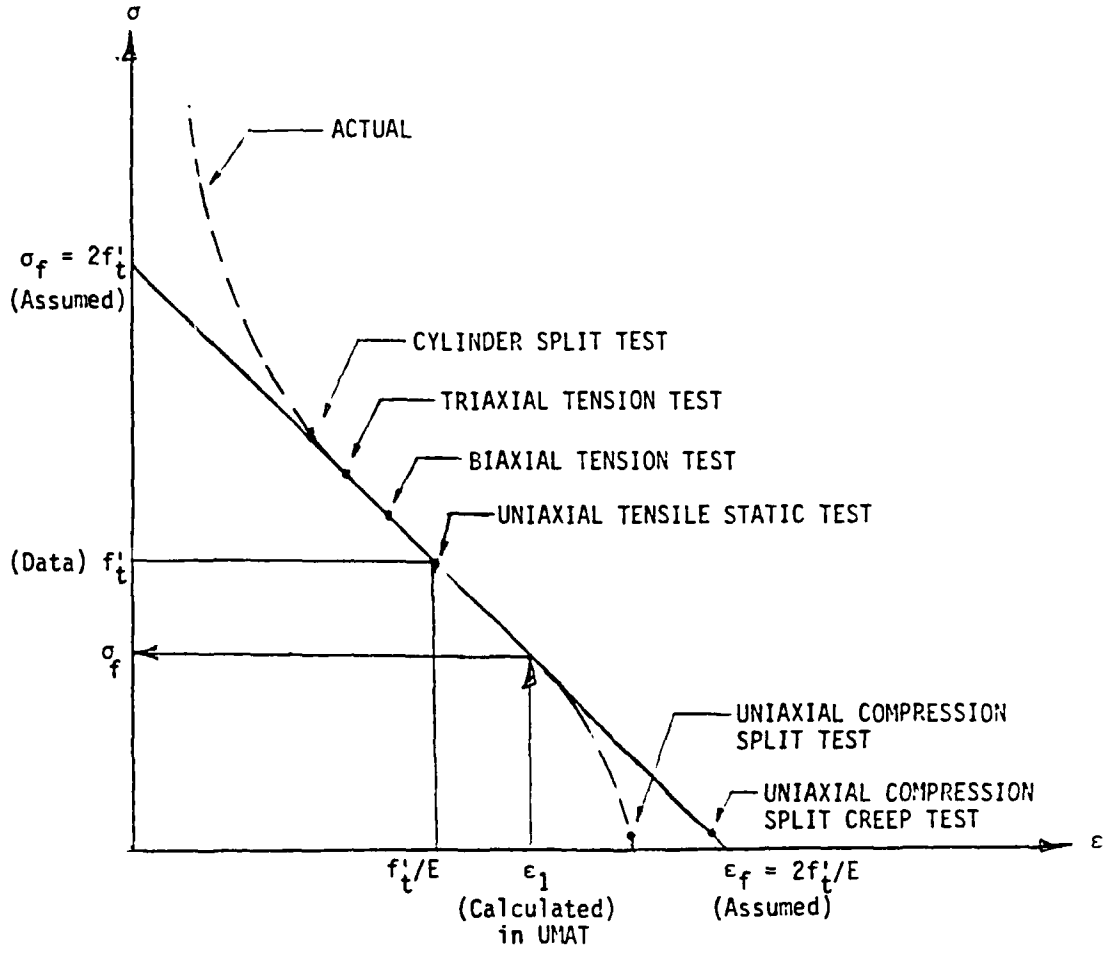

Figure 3. Interactive fracture criterion for concrete

Verification of the Aging Creep Model

9. To initially verify this model, two laboratory tests were simulated with the ABAQUS code. The first test was a creep test on silica-fume concrete and the second was a series of model overlay tests. Details of these verification problems are presented in the following sections. It should be pointed out that material properties for the silica fume, or overlay slab concretes are not suggested to be used for the lock wall overlay concretes. These verification studies were performed simply to develop confidence in the code and constitutive model.

10. The creep formulation used in the model was calibrated based on one creep test of silica fume concrete loaded at 3-day age. A 15-element, 24-node grid (Figure 4) was used to model silica fume concrete cylinders loaded in a uniaxial creep test apparatus. Runs were made in which cylinders were loaded to 40 percent of their ultimate compressive strengths at 1- , 3- , and 7-day ages. A comparison of the measured and calculated creep strains for the cylinders loaded at 3-day age (Figure 5) showed that the aging routine reasonably simulated the early-age creep response. The model allows the user to input a constant amplification factor for adjusting the magnitude of predicted creep strains for other loading ages. Results of runs using a factor of 1.46 for the 1-day data and 0.68 for the 7-day data showed calculated strains to be reasonably close to measure strains (Figures 6 and 7). Linear- and higher-order relationships between applied creep factors and age of concrete at loading can be developed as shown in Figures 8 and 9. An amplification factor for shrinkage strains can also be input in the model in a similar manner.

11. To verify the reasonableness of temperatures, stresses, and cracking predicted by the model, overlay slab tests were simulated. Actual shrinkage and creep curves for the concrete mix used in the slabs were obtained from 1-, 3-, 7-day ages, and control cylinders. Since thermal and shrinkage strains were of primary importance in modeling the slabs behavior, UMAT shrinkage predictions for a 6- by 16-in. cylinder were compared with test results, as shown in Figure 10. Shrinkage strains predicted by UMAT are based on data from 3-day silica fume cylinders. Actual strains (represented by the solid line) were approximately one half of predicted strains, and a shrinkage factor of 0.5 was input to UMAT in the final slab calculations. The slabs were models of concrete overlays, and consisted of two pours. The original pours were

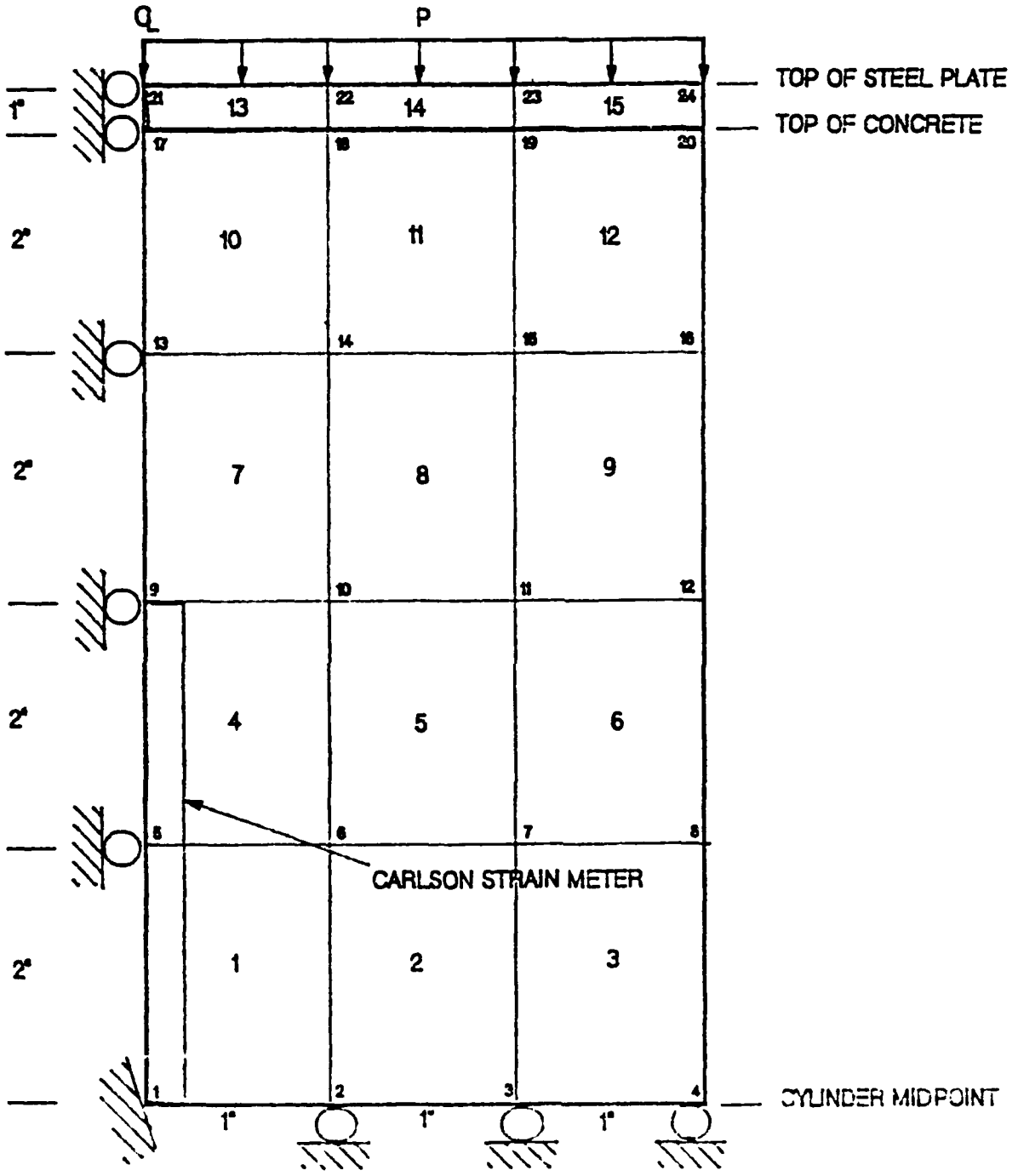

Figure 4. FE grid used to model silica fume concrete cylinders in creep test

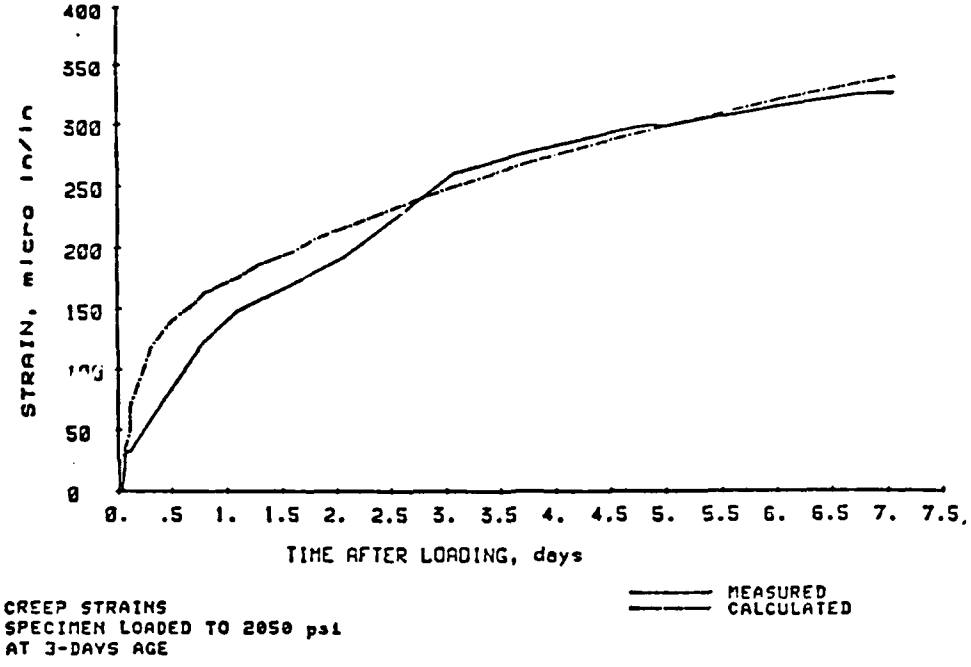

Figure 5. A comparison of measured and calculated creep strains for silica fume concrete cylinders loaded at 3-day age

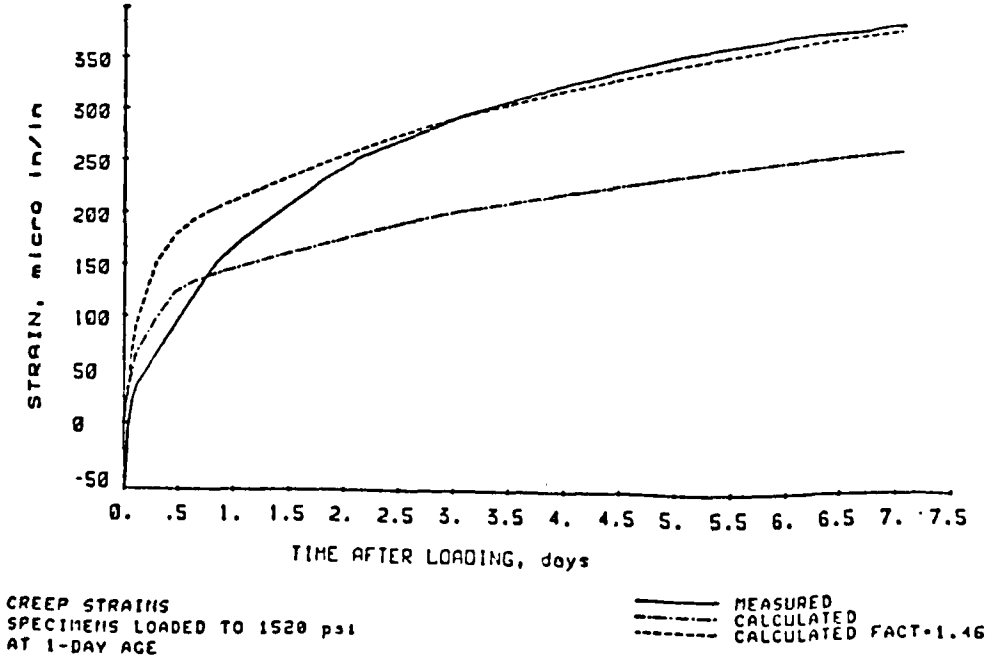

Figure 6. A comparison of measured and calculated creep strains for silica fume concrete cylinders loaded at 1-day age

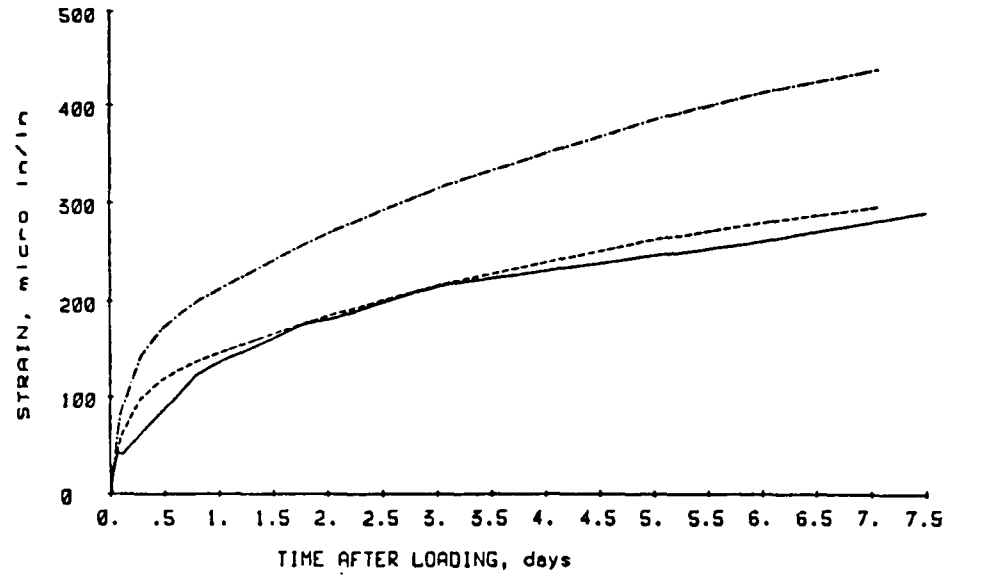

Figure 7. A comparison of measured and calculated creep strains for silica fume concrete cylinders loaded at 7-day age

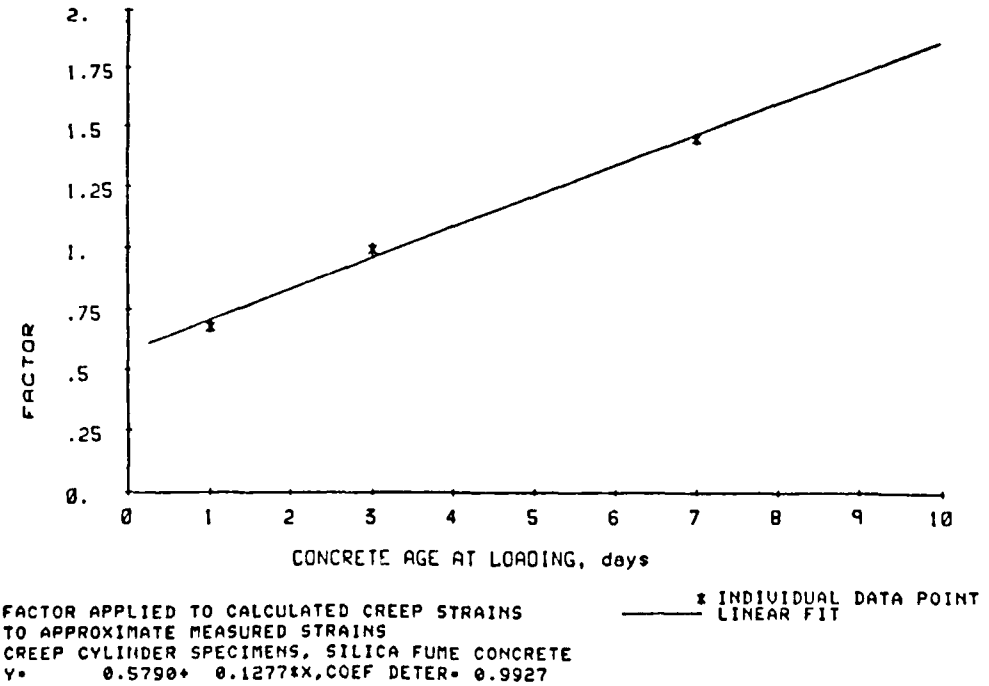

Figure 8. Relationship between creep factor and age of silica fume concrete at loading using a linear curve fit

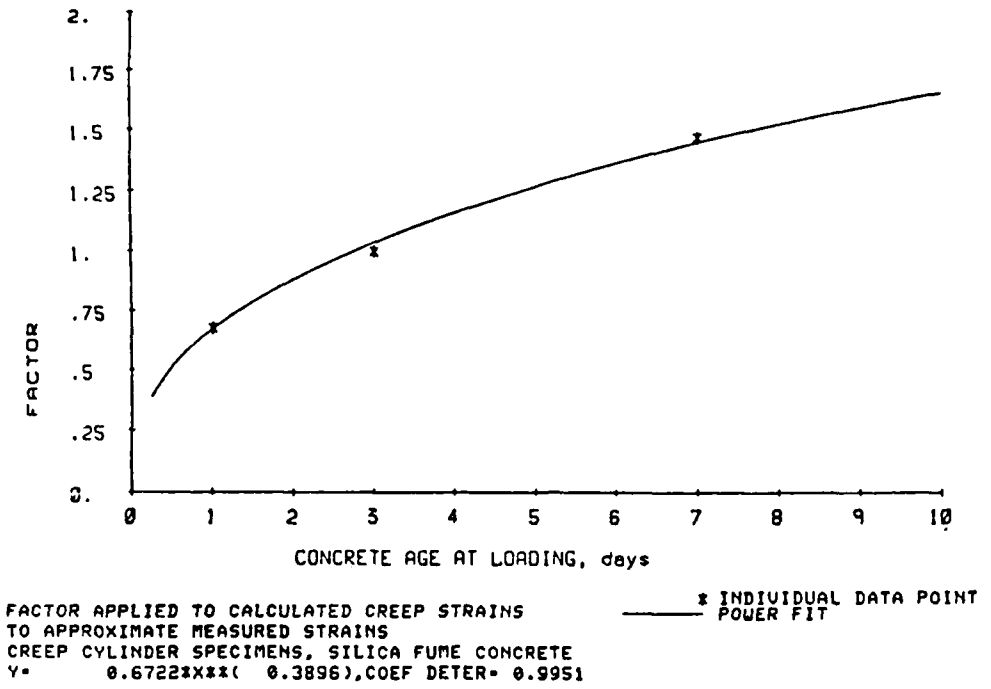

Figure 9. Relationship between creep factor and age of silica fume concrete at loading using a power curve fit

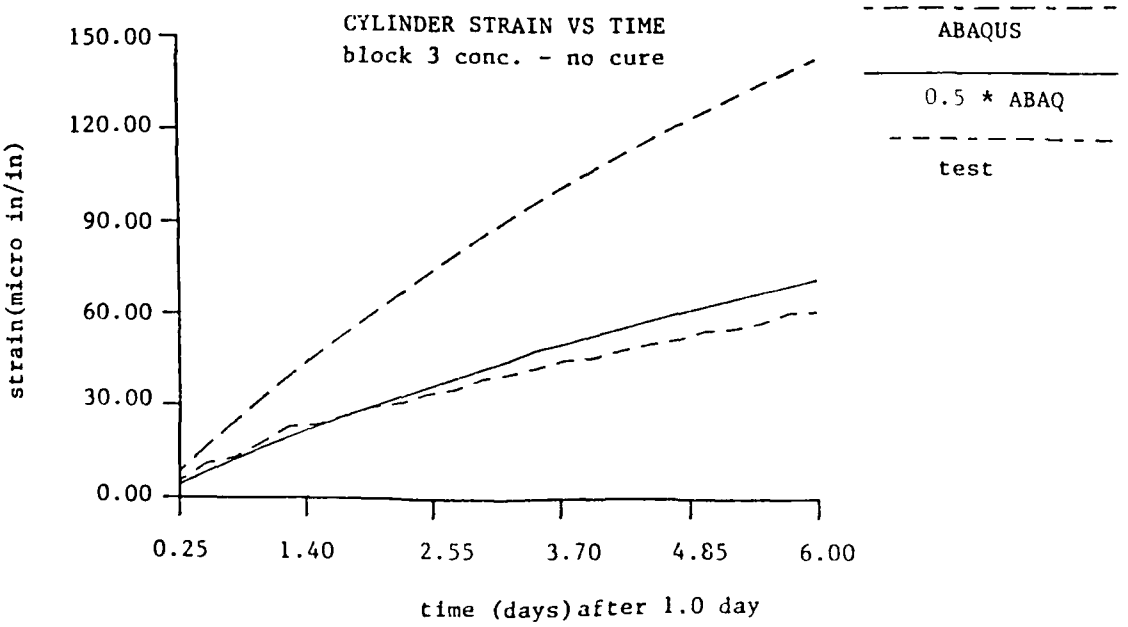

Figure 10. Cylinder shrinkage strain versus time

4 ft by 4 ft by 1 ft, and were allowed to age for approximately 60 days before the overlays were poured. The overlays for blocks 1 and 3 were 1 ft thick. Slab 5 had a 2-ft thick overlay. Forms were stripped from the overlays after 1 day. The slab 3 overlay was not cured, slab 1 was wet cured, and block 5 was covered with curing compound. A typical FE grid of a slab is shown in Figure 11. The grid represents one half of a slab. The first pour was modeled using 3- by 6-in., 4-node elements. The overlays were modeled using 3- by 3-in., 4-node elements. First, an ABAQUS heat transfer run was completed for each slab to determine temperatures throughout the overlays during the curing period. Temperatures generated in an insulated lift of a newly constructed lock wall were used to simulate the adiabatic temperature curve. Predicted temperatures were fairly close to actual recorded temperatures, as shown in Figure 12. Node 82 in the slab 5 model corresponded to the location of the thermocouple at the slab face (gage 14), and node 73 was located near the Carlson gage 2 in. from the face (gage 53). A final ABAQUS run was made for each slab using the UMAT subroutine. Predicted strains are compared with strains recorded by the Carlson meter in Figures 13 and 14. Strains calculated for block 1 are greater than recorded strains. Slab 1 was wet cured, and the film coefficient used in UMAT may not have adequately modeled the wet surface of the slab. Strains predicted for block 5 were very close to test strains. Cracks indicated by UMAT for block 3 at 7 days are shown in Figure 15. All cracks in the FE model occurred at the interface between the old concrete and the overlay. This is the expected response for an overlay poured in midsummer. The predicted crack spacing is a result of the smeared crack approach to modeling concrete behavior. Cracks can occur only at integration points and will occur at each integration point when the "cracking strain" is exceeded at that point.

Finite Element Grid for Lock Wall Resurfacing Slab

12. A 2-D formulation was used in analyzing the lock wall cracking problem. The 2-D assumption was justified based on field observations of cracks (Figure 1) which appeared to be insensitive to gravity stresses and on the fact that the temperature is expected to be quite uniform in the vertical dimension. After different mesh densities and element types were evaluated based on computational efficiency and accuracy of results, the grid shown in

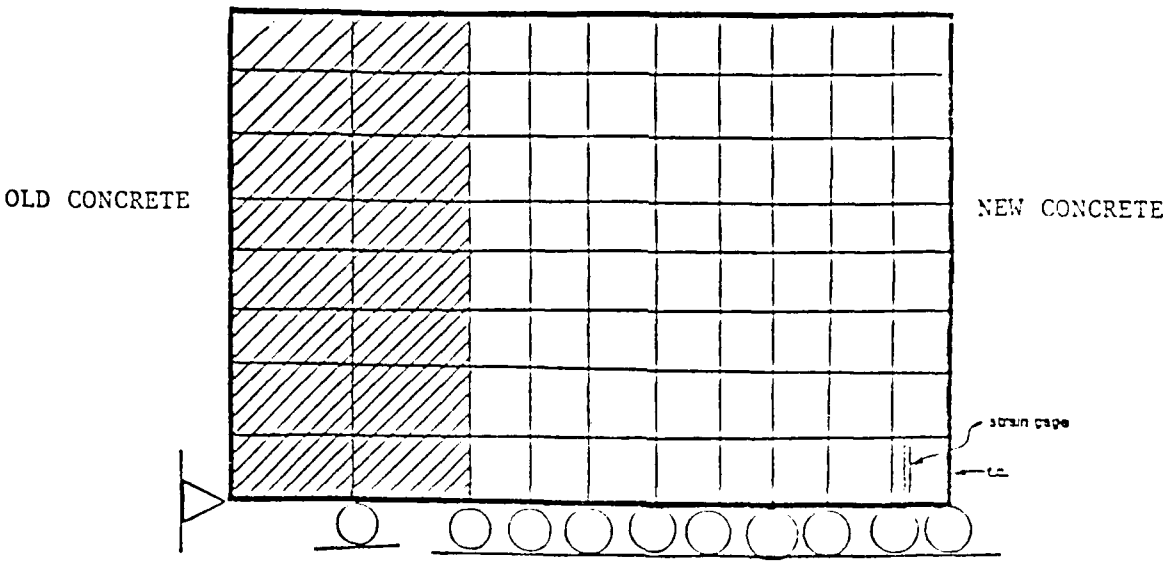

Figure 11. FE grid of overlay slab

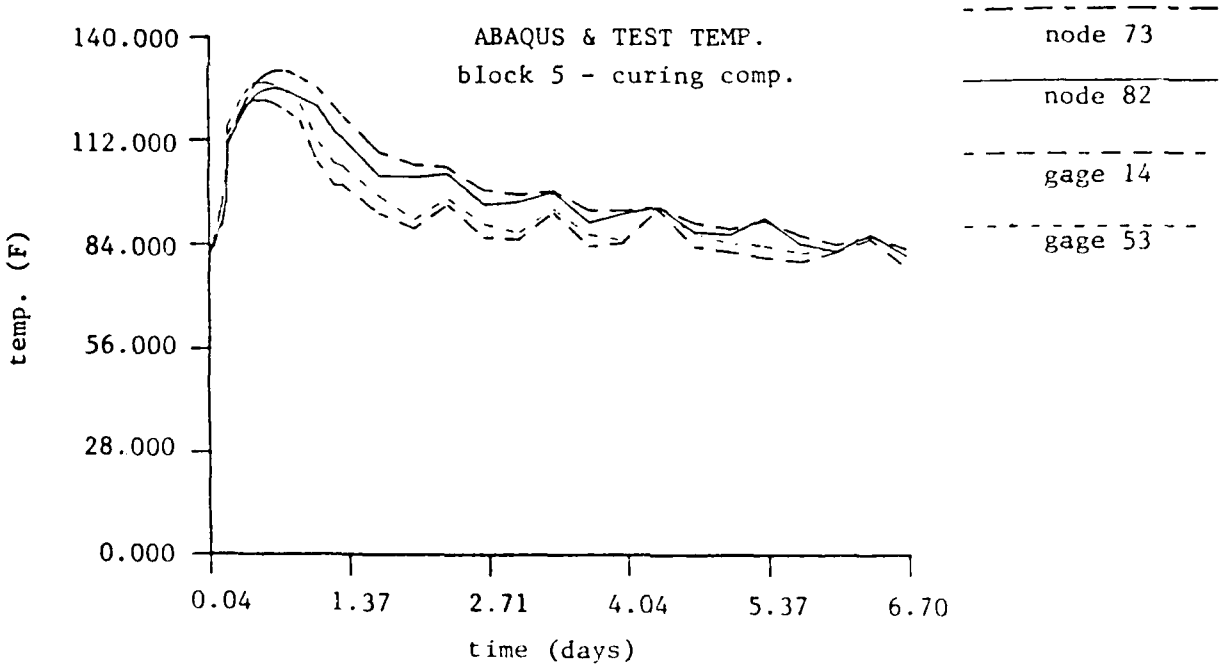

Figure 12. Abaqus and test temp

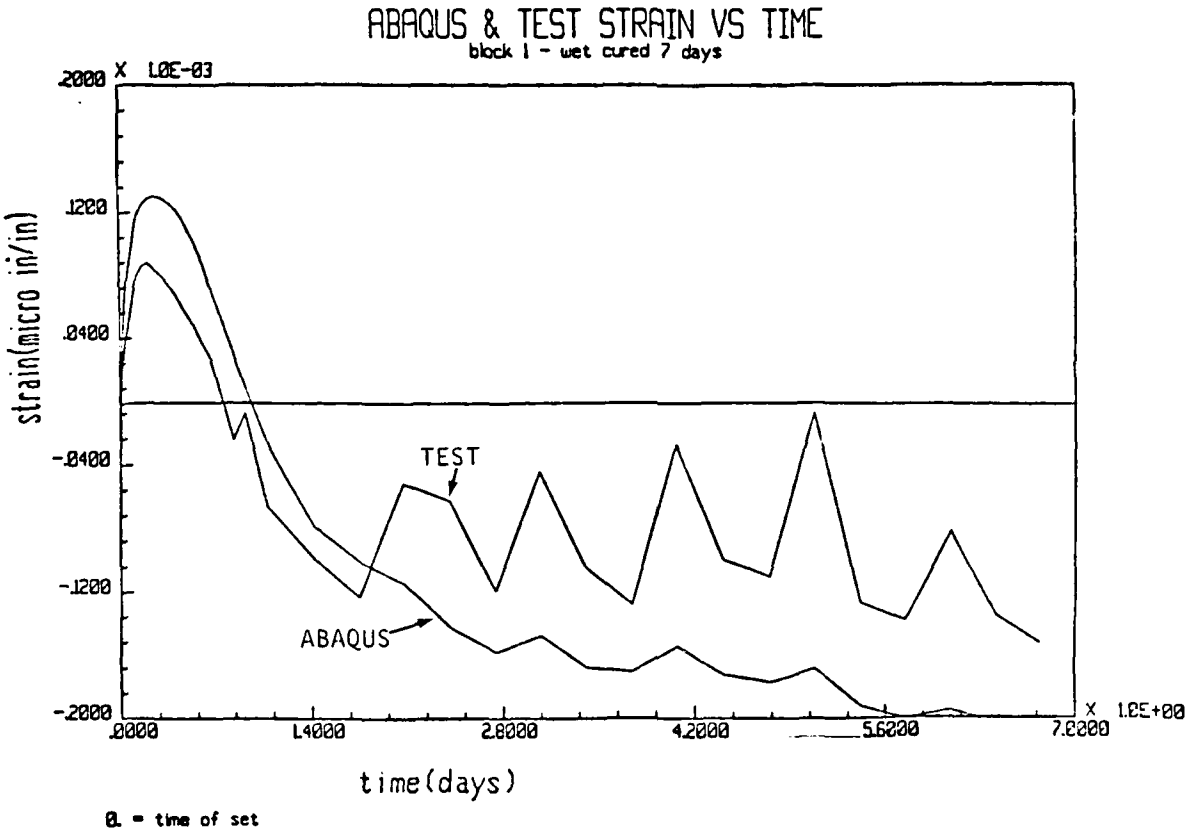

Figure 13. Abaqus and test strain versus time

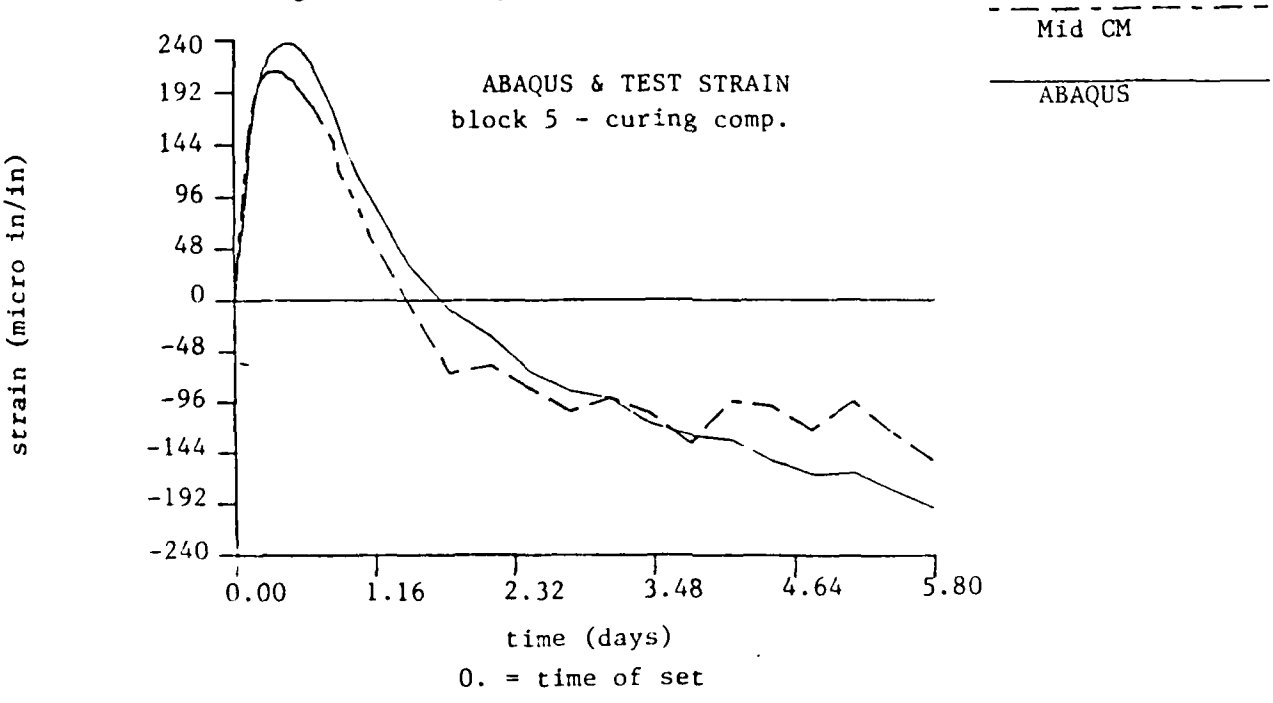

Figure 14. Abaqus and test strain

Figure 16 was selected for the lock wall analysis. The element used is defined in ABAQUS as CEP4 and is a 4-node plane strain quadrilateral. Geometric details and boundary conditions for the FE grid are presented in Figure 17.

Analysis Procedure

13. The thermal stress analysis problem is initiated by specifying the internal heat generated by the freshly placed concrete during the hydration process. This heat generation is defined in ABAQUS by a heat flux array and is determined here from the adiabatic temperature curve for the new concrete used at Lock and Dam No. 1. The discretized heat conduction equations are then solved consistent with the imposed thermal boundary conditions to determine the temperatures throughout the FE grid as a function of time. Strains and stresses throughout the grid are then calculated consistent with the imposed mechanical boundary conditions. Effects of shrinkage and creep are included in the analysis by specifying shrinkage versus time and specific creep-strain curves for concrete loaded as early as 1 day. Cracking is considered by specifying a concrete tensile strain capacity such that when the principal tensile strain at a particular integration point reaches this specified value, a crack is formed normal to the direction of the principal strain. This crack is assumed to be smeared over the tributary area of the element associates with the integration point.

Lock and Dam No. 1 - Baseline Problem

14. The baseline problem (BP) is defined here as the FE solution which best represents the L&D No. 1 resurfacing problem based on field conditions and available material properties. The field conditions were:

a. An ambient (reference) temperature of 50° F.

b. 216- by 180- by 18-in. resurfacing slab.

c. A 3/4-in. plywood form which remained in place for the duration of the analysis.

d. A No. 6 rebar mat with bars spaced at 12 in. O.C. and No. 8 dowels at 36 in. O.C.

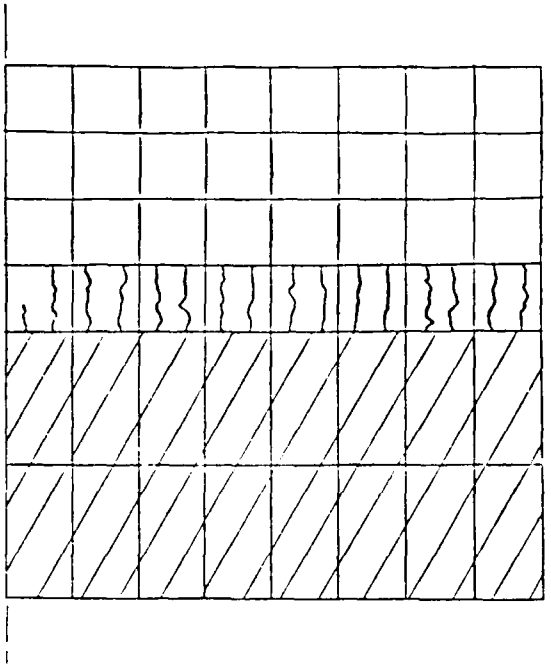

Figure 15. Block 3 cracking at approximately 7 days after set

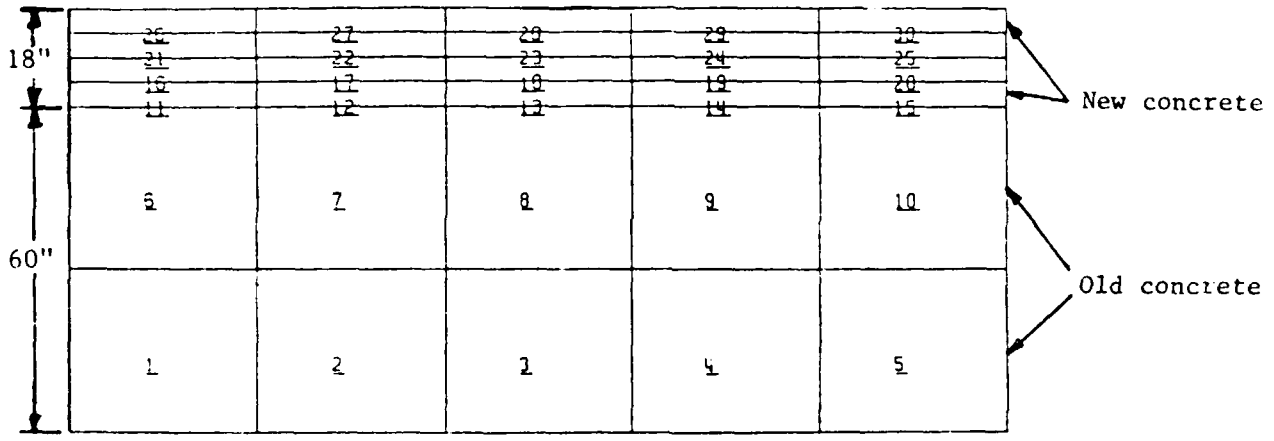

a. Element numbers

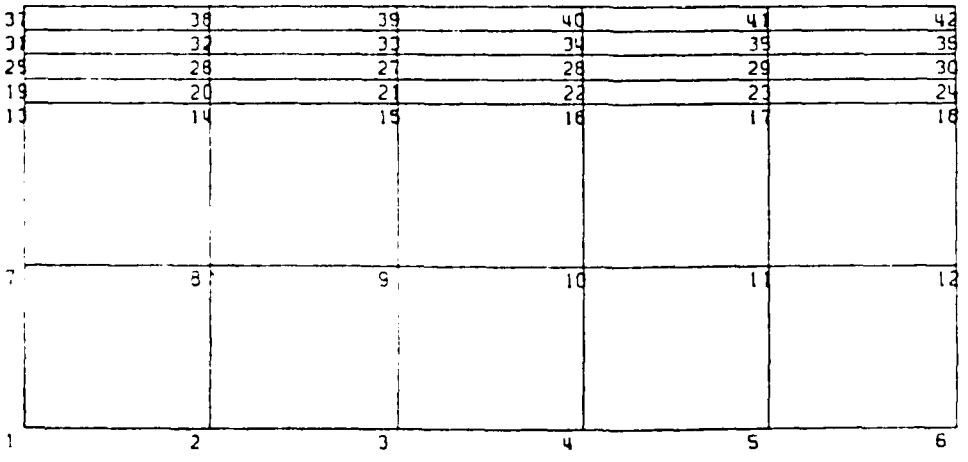

b. Node numbers

Figure 16. FE grid

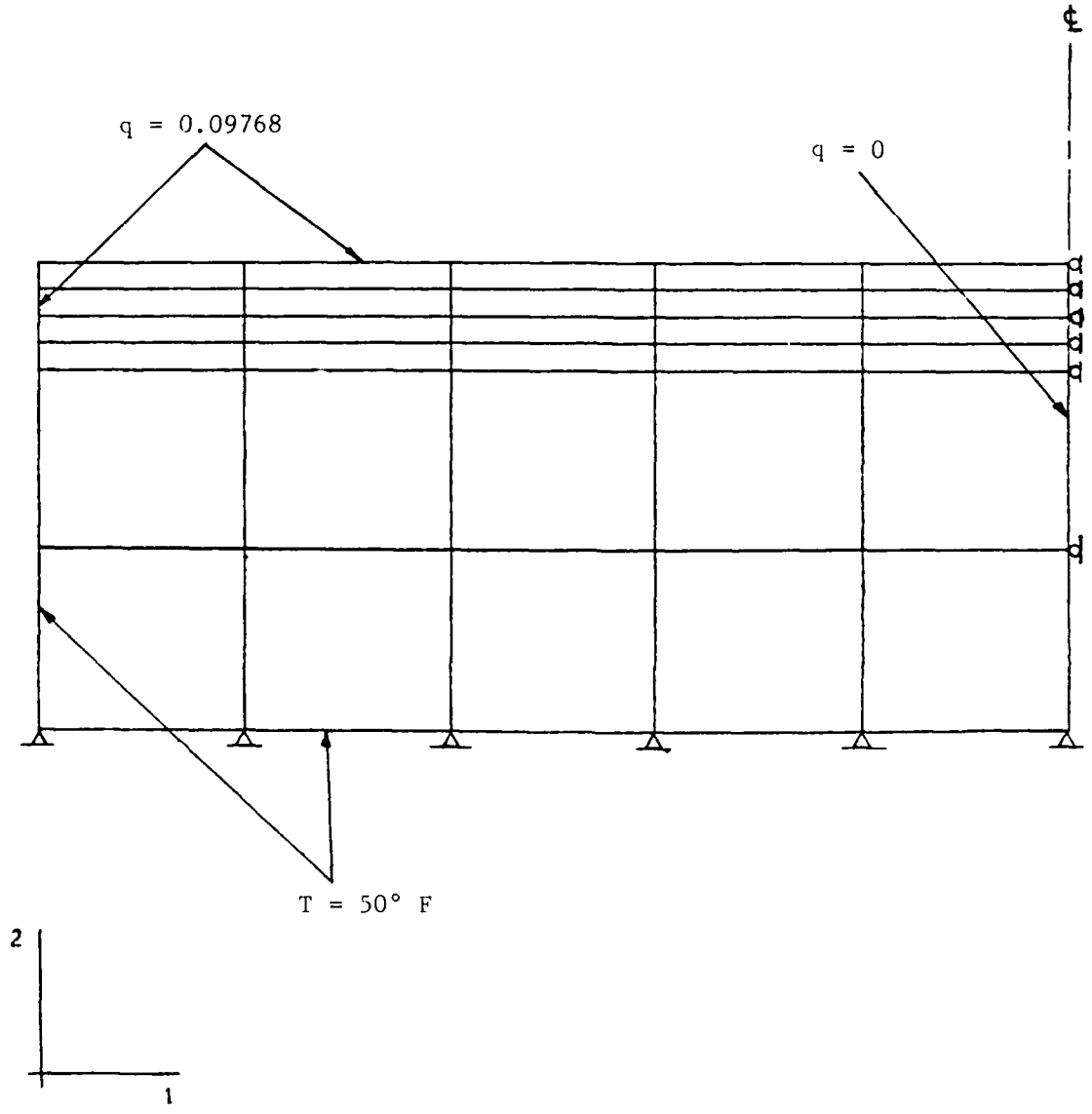

Figure 17. Boundary conditions for thermal stress analysis of baseline problem (Heat transfer (q) in units of: Btu/day (sq in. × ° F)

15. The material properties for the new concrete consisted of:

a. Modulus of elasticity variation with time as presented in Figure 18 and Table 1.

b. Tensile strain capacity and modulus of rupture variation with time as presented in Table 2.

c. Thermal properties and average 28-day mechanical properties presented in Table 3.

d. The adiabatic temperature curve presented in Figure 19.

16. Using the input data presented above, the thermal stresses and strains are calculated at each integration point for a period of 5 days. The solution time step ranged from 2 hr during the first day to 24 hr during the fifth day. The results of the analysis were studied first by evaluating stress contour plots at critical time increments as shown in Figures 20 and 21. The sequence of contour plots in these figures indicates where high tensile stresses are beginning to localize and where cracks form and stresses are redistributed. After critical regions are located from the stress contour plots, the actual stress time histories for typical integration points in these regions can be plotted as shown in Figure 22. From the time-history plots, it is seen that the concrete initially goes into compression due to the combination of thermal expansion and the restraint provided by the old concrete. The compression stresses decrease due to the combination of declining temperature in the new concrete and shrinkage of the new concrete. As this process continues, cracks form and stresses normal to the crack planes are reduced to zero.

17. The contour plots shown in Figures 20 and 21 and the stress time-history plots presented in Figure 22 represent analyses where upper-bound and lower-bound shrinkage is simulated. The parameters defining shrinkage bounds were developed from data taken from the American Concrete Institute* and presented in Figure 23. The significant effects of shrinkage are seen in Figure 22 in that the lower-bound curve resulted in no cracking in 5 days. However, it was seen that cracking would occur even for the lower-bound curves at later times. It should be noted from Figure 23 that these curves are for shrinkage occurring after 7 days. Very little test data are available for

---

* American Concrete Institute. 1970. "Designing for Effects of Creep, Shrinkage, Temperature in Concrete Structures," ACI Publication SP-27, Detroit, Mich.

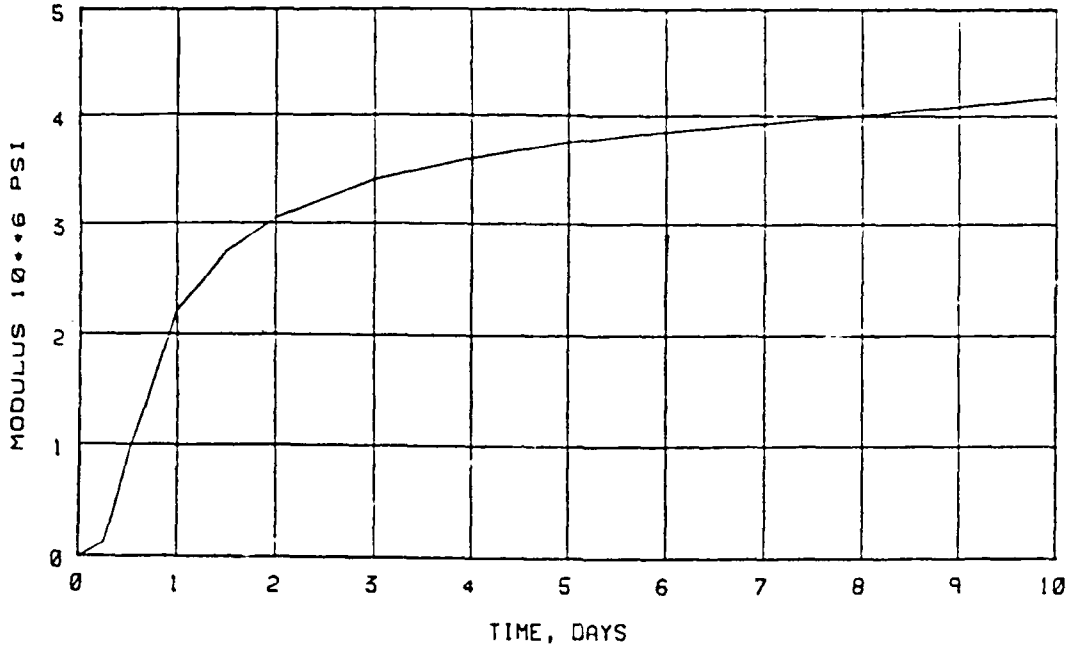

Figure 18. Modulus of elasticity versus time

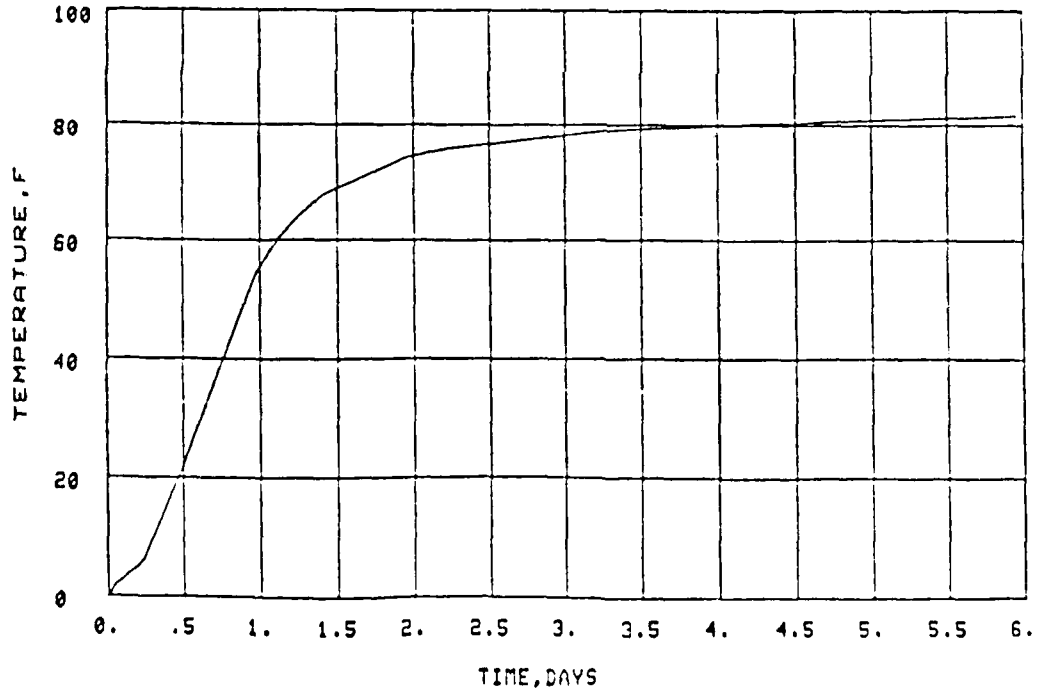

Figure 19. Adiabatic temperature rise versus time

Table 1

Results from Unconfined Compressive Strength Tests

Age days	Poisson's Ratio	Ultimate Strength psi	Modulus of Elasticity psi
1	0.16	2,620	3,350,000
3	0.17	3,850	4,050,000
7	0.20	4,380	4,250,000
14	0.19	5,010	4,500,000
28	0.18	5,810	4,800,000

Table 2

Results from Strain Capacity Tests

Age days	Modulus of Rupture psi	Strain Capacity at 90% Mod of Rupture		Modulus of Elasticity at 40% Mod of Rupture psi
		Tensile micro in./in.	Compressive micro in./in.	
1	370	106	96	3,900,000
3	441	102	108	3,600,000
7	438	103	97	4,500,000
14	545	121	111	4,850,000

Table 3

Concrete Properties at 28-day Age

Property	Value
Ultimate strength	5,740 psi
Modulus of elasticity	4,800,000 psi
Poisson's ratio	0.19
Density	1.46 pcf
Specific heat	0.22 Btu/lb (deg F)
Diffusivity	126.2 sq in./day
Conductivity	2.354 Btu/day/(deg F)
Coefficient of thermal expansion	0.000005 in./deg F

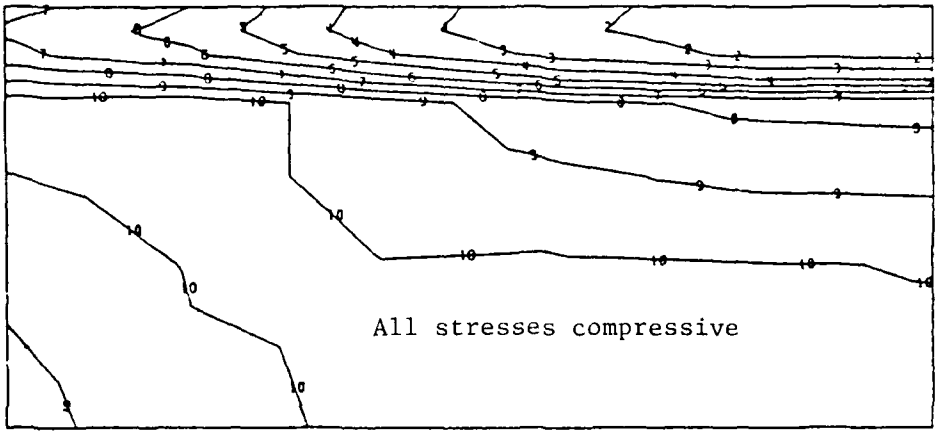

a. T = 0.1667 day

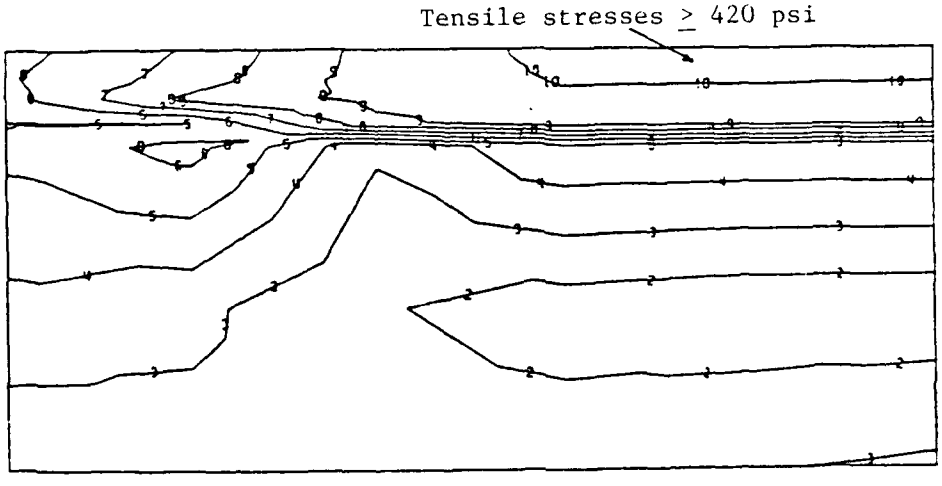

b. T = 3.0 days

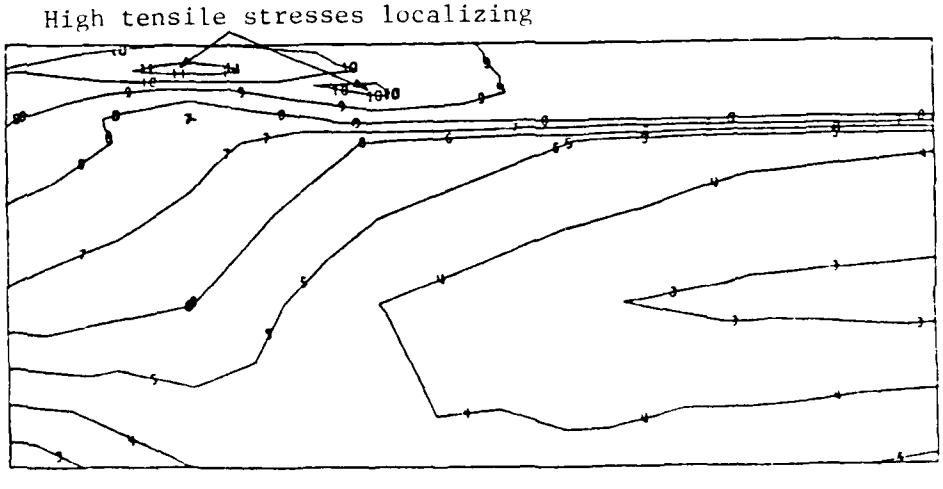

c. T = 3.5 days

Figure 20. Stress contour plots of stresses in the 1 or horizontal direction from analysis using upper-bound shrinkage

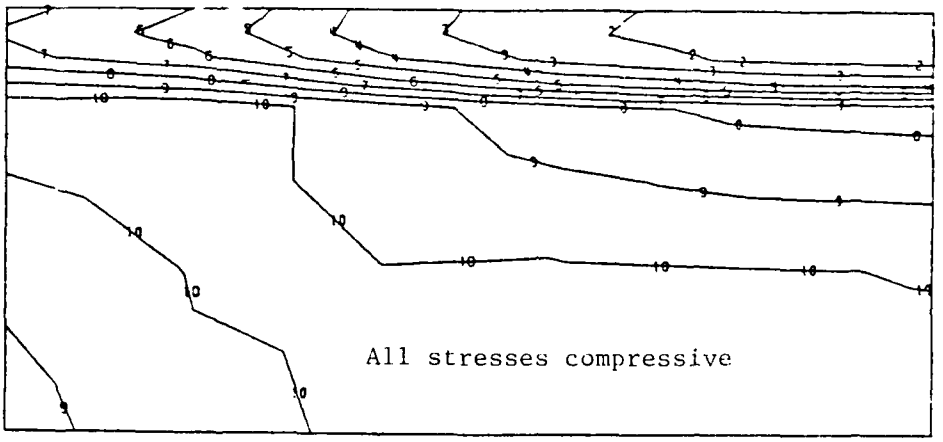

a. T = 0.1667 day

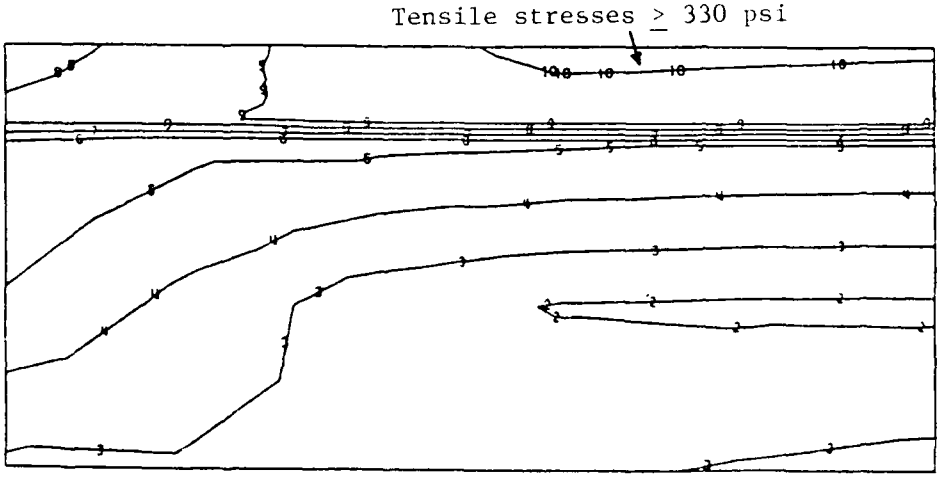

b. T = 5.0 days

Figure 21. Stress contour plots of stresses in the 1 or horizontal direction from analysis using lower-bound shrinkage

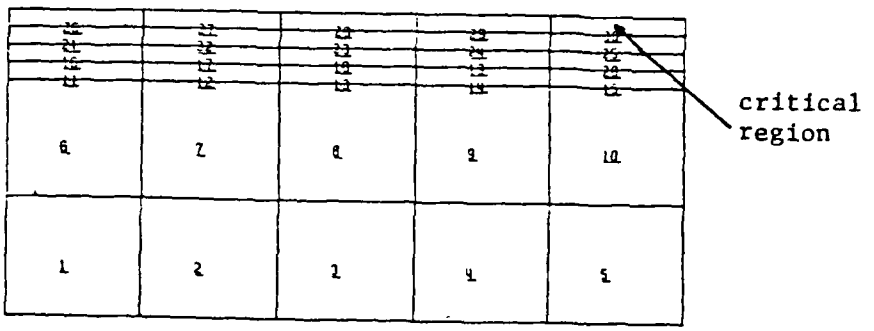

a. FE grid

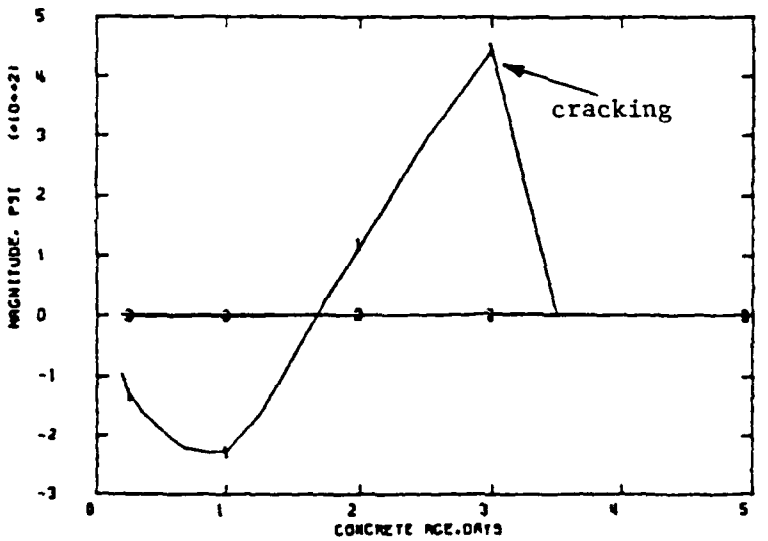

b. Upper-bound shrinkage

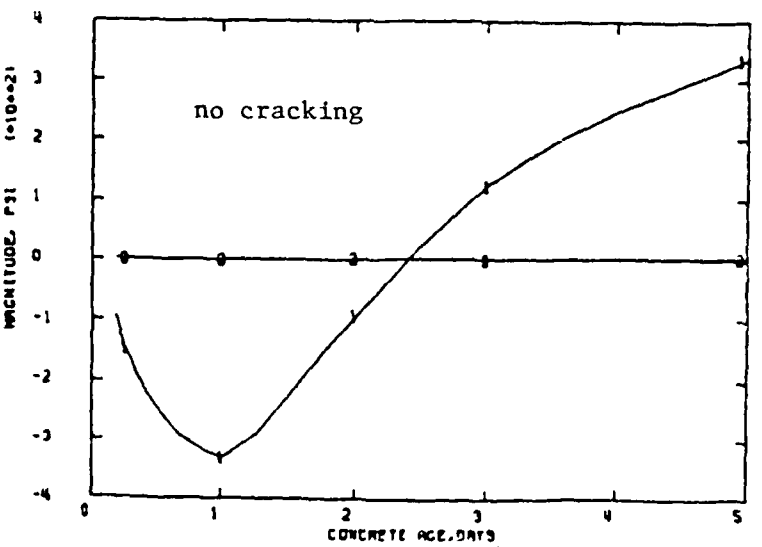

c. Lower-bound shrinkage

Figure 22. Stress-time histories at critical regions for baseline problem

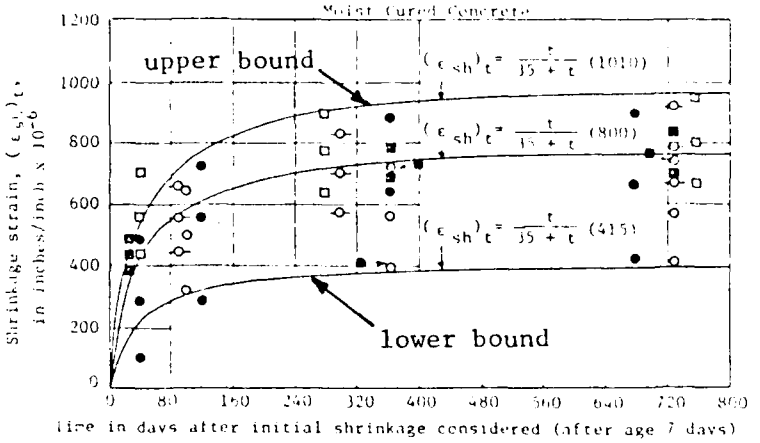

Figure 23. Shrinkage strain versus time for moist cured concrete (from ACI (1970))

shrinkage of concrete at early times (i.e., 1 day). However, a limited number of tests were conducted at WES which compared favorably with the results of Slate and Mathews* at approximately 1 day. This assumed isotropic shrinkage was very high and is being further evaluated before incorporation into the model. Reference curves for elasticity, creep, and shrinkage were developed to define the generalized response of the model with time. Amplification of responses was controlled through input parameters. Data used to develop curves came from test data of silica fume concrete as previously discussed and are presented in Figures 24 and 25.

* F. O. Slate and R. E. Matthews. 1967 (Jan). "Volume Changes on Setting and Curing of Cement Paste and Concrete from Zero to Seven Days," Journal, American Concrete Institute, No. 64-4.

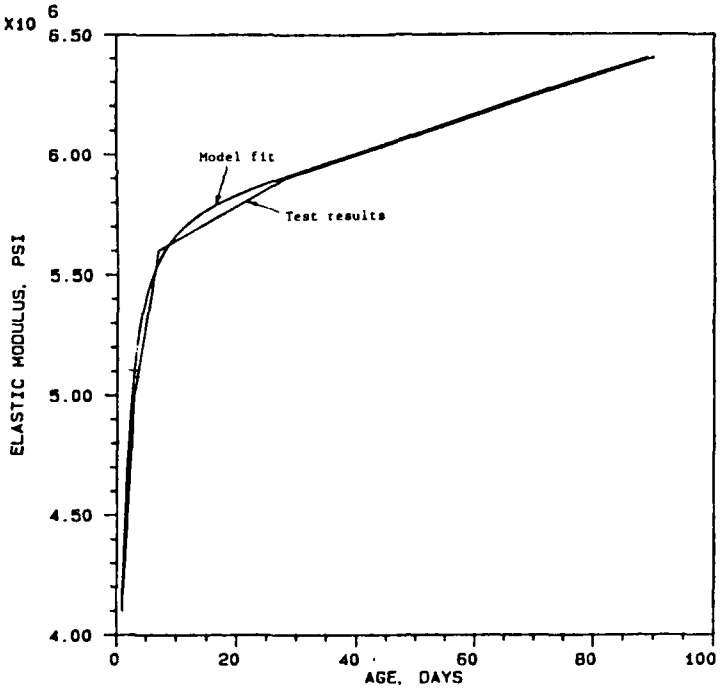

a. Elastic modulus of concrete as a function of age

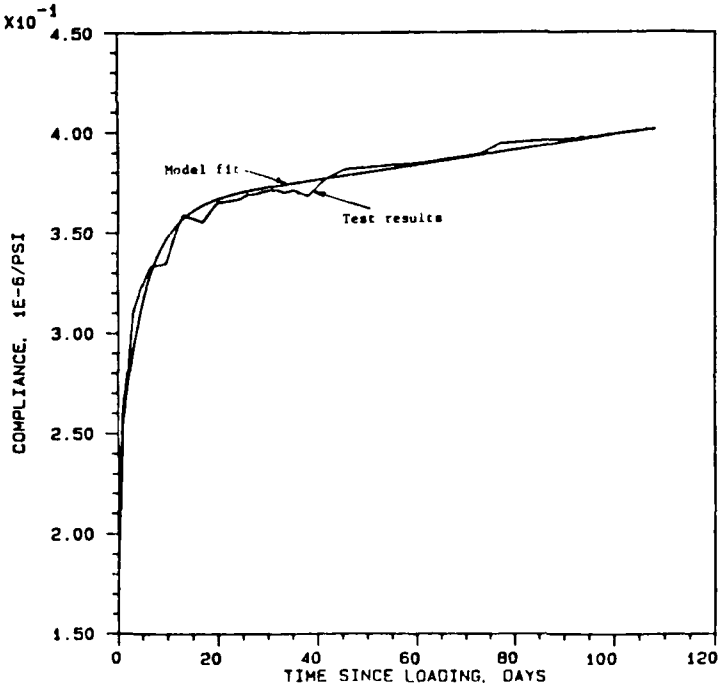

b. Elastic and creep response of concrete: Age = 3 days

Figure 24. Elastic modulus and specific creep strain for silica fume concrete tested at WES

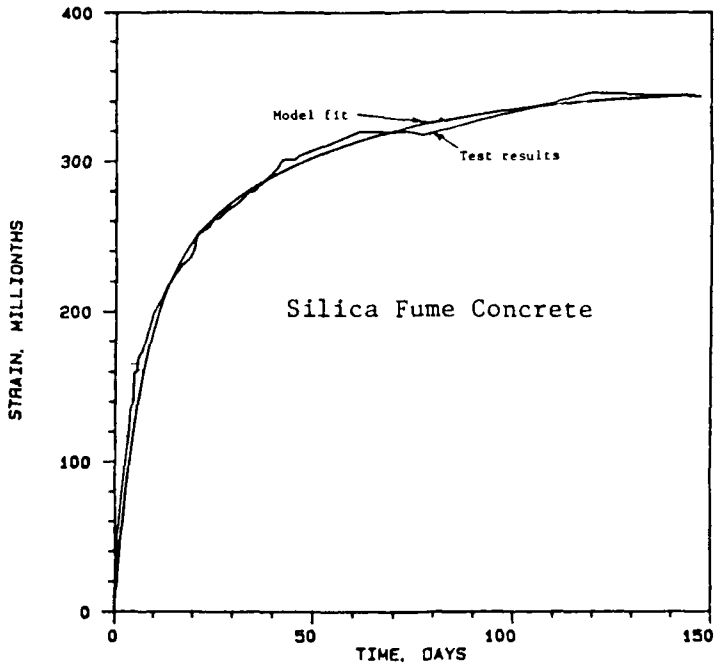

a. Shrinkage for concrete at 3-day age

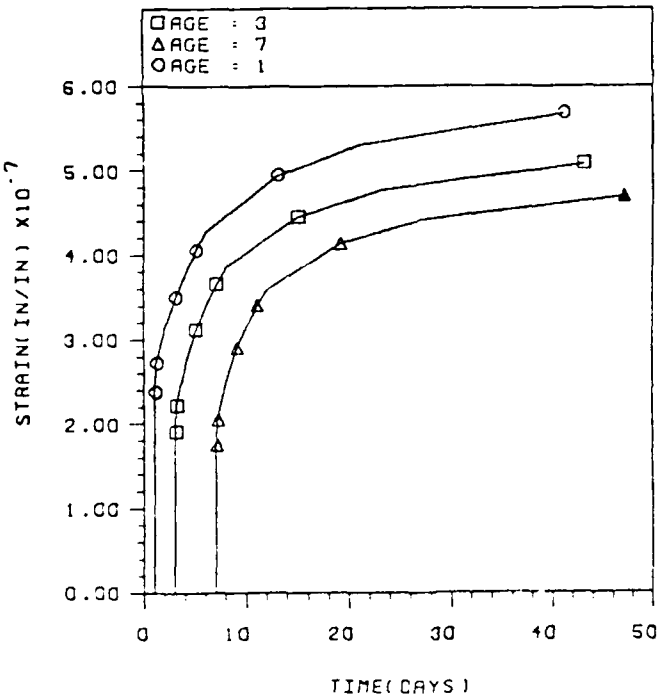

b. Total creep strains predicted by model for silica fume concrete tests

Figure 25. Shrinkage and creep strains for silica fume concrete test at WES

PART III: PARAMETER STUDIES

Aging Creep Model Analyses

18. After the aging creep model was refined based on limited laboratory tests, several analyses were conducted with varying parameters which can significantly affect stresses in the lock wall resurfacing problem. These parameters included: temperature of the new concrete at placement, temperature of the old concrete at placement, form insulation, providing a bond breaker at old-new concrete interface, form removal time, and the effects of providing dowels and reinforcing steel. Founded on the results of the baseline problem, it was decided that the effects of varying key parameters could best be determined by studying stress-time histories at a critical element. This element is number 30 (Figure 16) and the stress component is in the 1 or horizontal direction. In addition to the parameters evaluated in this section grid size, boundary conditions and solution time-step size were evaluated. None of these parameters had significant effects on stress distributions or times of cracking, and these results are not discussed herein.

Placement Temperatures

19. Placing concrete with temperatures of 50° F and 40° F resulted in stress time histories as shown in Figure 26. Compressive stresses were reduced for the lower placement temperatures. However, tensile cracking still occurred at approximately 3 days. Although it is generally accepted that lower placement temperature decreases thermal contraction, the feasibility and economy of cooling concrete before placement must be considered.

Temperature of Old Concrete

20. The temperature of old concrete when varied between 50° F and 60° F had little effect on cracking within the resurfacing slab (Figure 27). However when wider ranges of old concrete and ambient temperatures were studied, the effects of extreme conditions were more significant. A number of FF runs (Table 4) were made to determine if extreme ambient temperatures would result in cracks developing in the concrete resurfacing of the lock wall model.

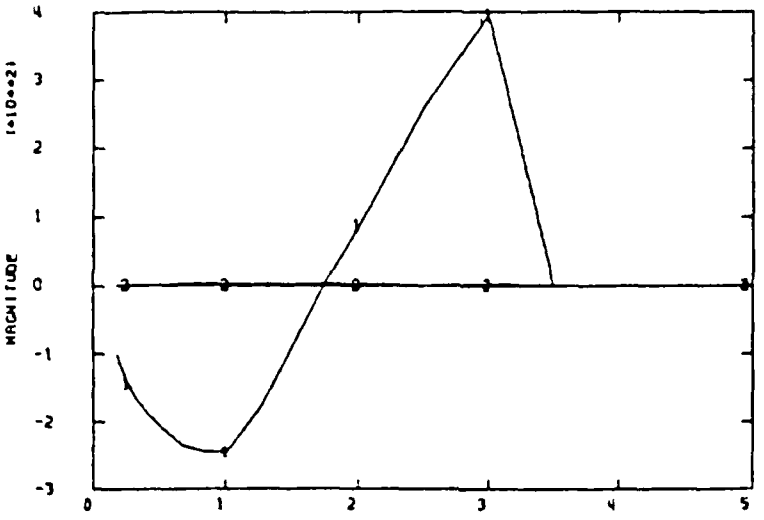

a. Placement temperature, T = 50° F

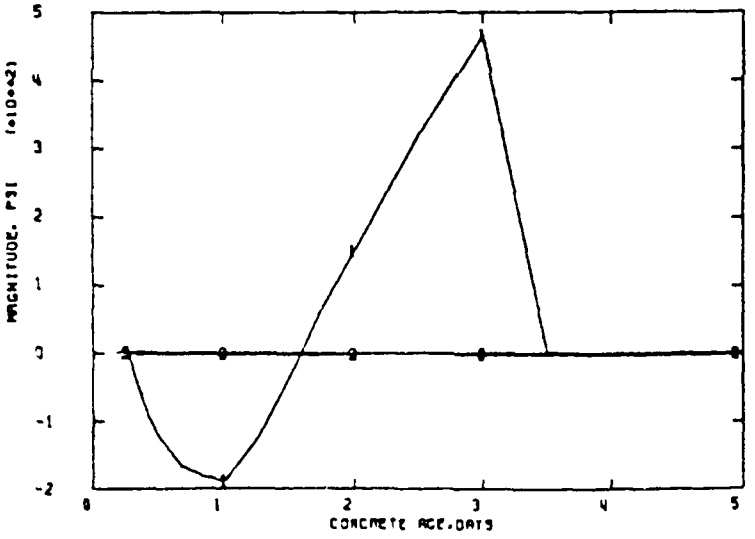

b. Placement temperature, T = 40° F

Figure 26. Effects of placement temperature on stress-time histories (stresses predicted at element 30)

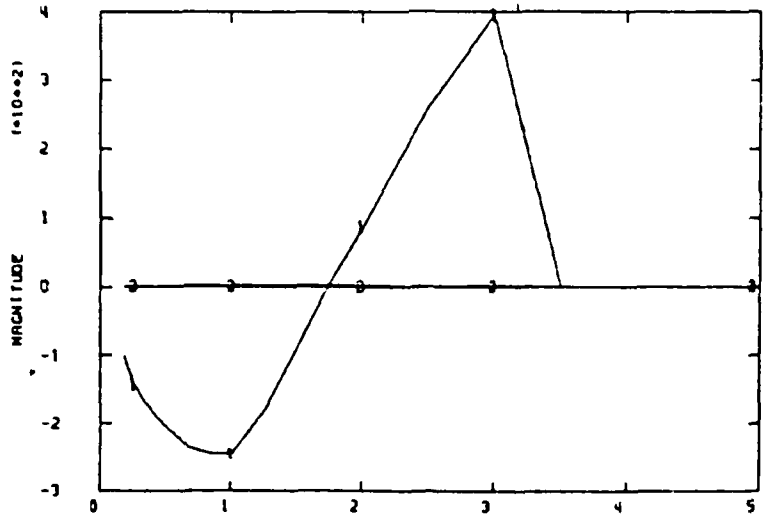

a. Old concrete temperature, T = 50° F

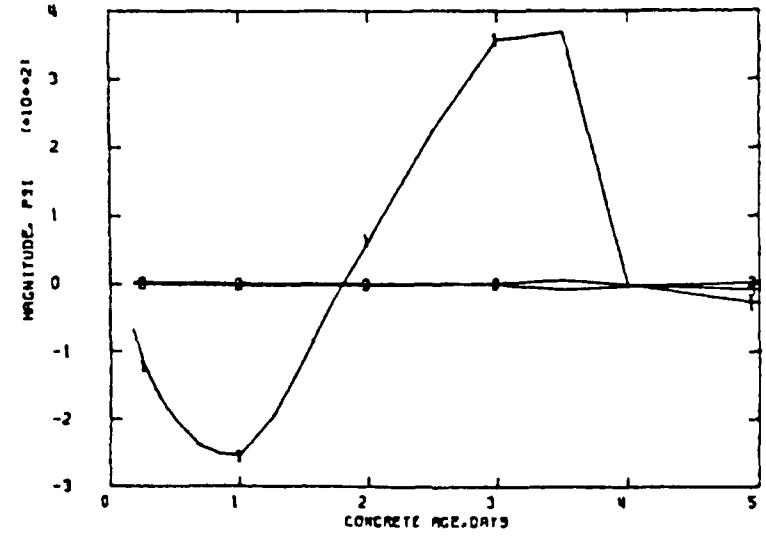

b. Old concrete temperature, T = 60° F

Figure 27. Effects of temperature of old concrete on stress-time histories (stresses predicted at element 30)

Table 4

Effects of Extremes in Ambient Temperatures on Cracking in Lock Wall Resurfacing Concrete

EARLY-AGE CRACKING OF LOCK WALL RESURFACING CONCRETE AS COMPUTED BY 'ABAQUS' FE PROGRAM (ANALYSIS FOR FIRST 5 DAYS AFTER PLACEMENT)**

Run	Ambient Temp F	Exposure Time day	Shrinkage Rate Factor	Age at Cracking day
R1U	50	0-1*	0.0	NC
	50	1.25-5		
R1U	50	0-1*	1.0	3.00
	50	1.25-5		
R1V	50	0-1*	0.0	5.00
	25	1.25-5		
R1V	50	0-1*	1.0	2.50
	25	1.25-5		
R1W	50	0-1*	0.0	2.00
	0	1.25-5		
R1W	50	0-1*	1.0	1.75
	0	1.25-5		
R1UU	50	0-5*	0.0	NC
R1UU	50	0-5*	1.0	4.00
R1UUU	70-100	0-1*	0.0	NC
	70-100	1.25-5		
R1UUU	70-100	0-1*	1.0	2.33
	70-100	1.25-5		
R1UUU	100	0-1*	0.0	NC
	100	1.25-5		
R1UUU	100	0-1*	1.0	2.67
	100	1.25-5		

* Exposed faces insulated by 3/4-in. thick plywood forms.

** Note that concrete placement temperature was assumed to be 60° F and the resulting computed temperature of 67° F for the concrete at assumed time of set (6 hr after placement) was used as the stress-free temperature for all analyses.

Results of a run in which the ambient temperature was set to 50° F and no shrinkage effects included showed that no cracks developed within the 5-day analysis period. The inclusion of the effects of shrinkage in this analysis resulted in cracks developing at the surface of the resurfacing concrete 3 days after placement. Results of runs using ambient temperatures of 25° and 0° F and no shrinkage effects included showed cracks developing at the surface of the resurfacing concrete at times of 5 and 2 days after placement, respectively. The inclusion of shrinkage effects in the analyses showed cracks developing at earlier times. Two other runs were made in which the ambient temperature was set at 50° F and the forms left on the face of the resurfacing for the duration of the analysis. These results showed cracks developing at the surface of the resurfacing concrete only for the run that included shrinkage effects. For all other runs, the forms were removed at the end of the first day.

21. Sets of runs were made using ambient temperatures cycled between 70 and 100° F over 24-hr periods, and ambient temperature held constant at 100° F for the duration of the analysis. The results for both temperature conditions showed cracks developing only when shrinkage was included in the analyses. The location of the cracking for the cold ambient temperatures was at the lock face (Figure 28), whereas the location of the cracking for the high temperatures was at the interface between the old and the new concretes near the monolith joint (Figure 29).

Form Insulation

22. Providing form insulation increases the magnitude and duration of the compressive stress in the new concrete (Figure 30). Also, the time of cracking was progressively increased as higher insulation values were assumed. Although no cracks were predicted for the 5-day period of analysis, it can be seen from Figure 30c that cracking was imminent.

Bond Breaker

23. The effects of assuming a bond breaker (i.e., a low-friction restraint between the old and new concrete) can be seen in Figure 31. The magnitude of stresses are reduced to a level in which cracking would not

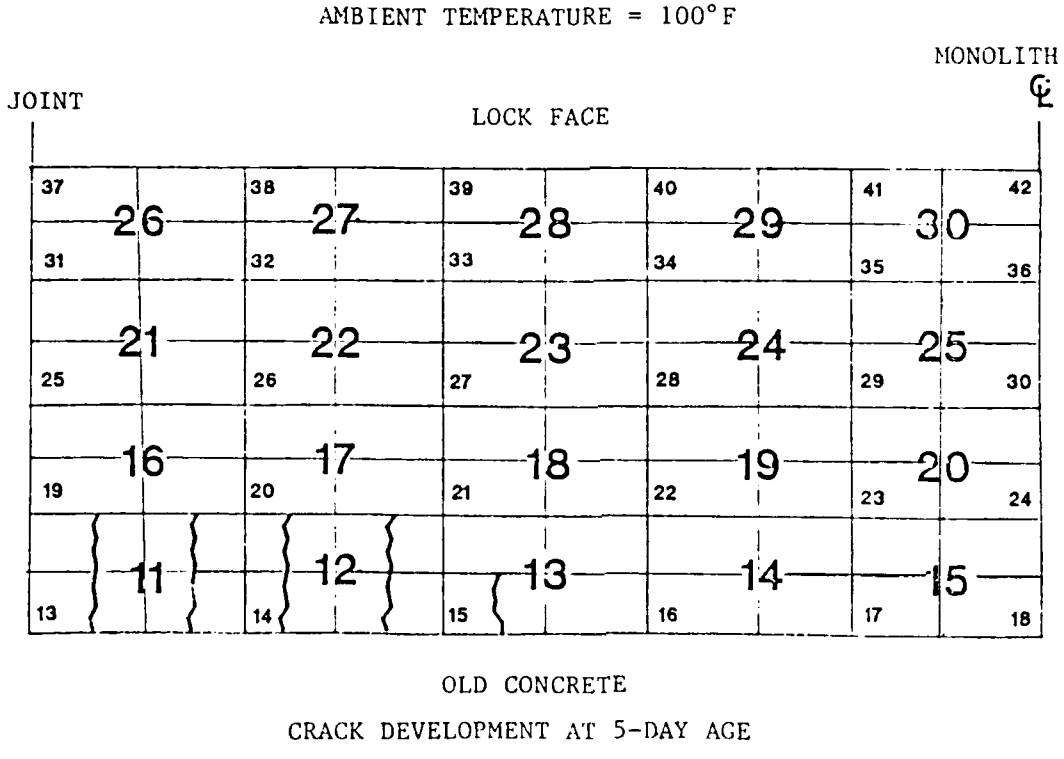

Figure 28. Predicted cracking in lock wall resurfacing concrete due to cold temperatures with shrinkage effects included

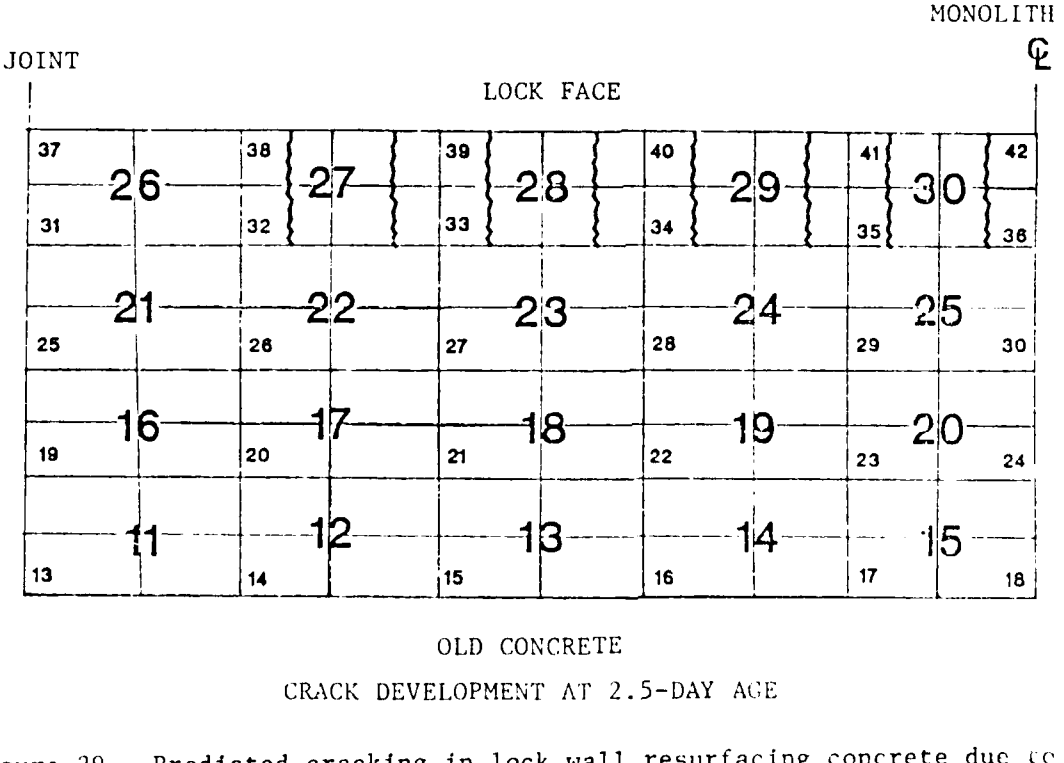

Figure 29. Predicted cracking in lock wall resurfacing concrete due to hot temperatures with shrinkage effects included

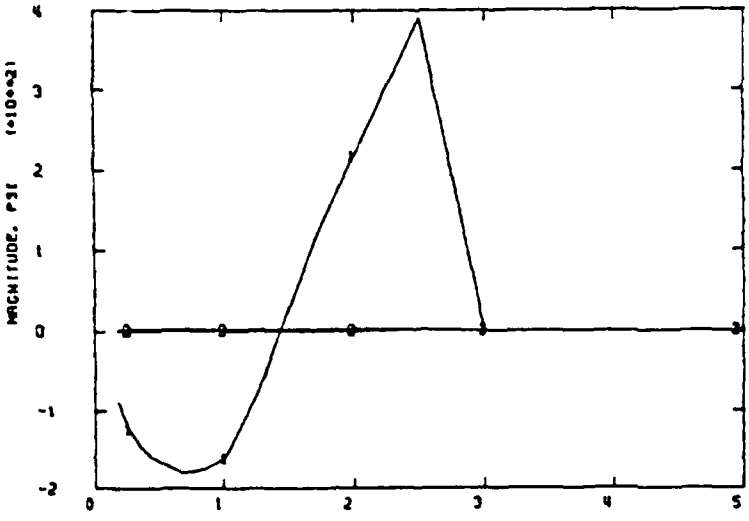

a. No insulation

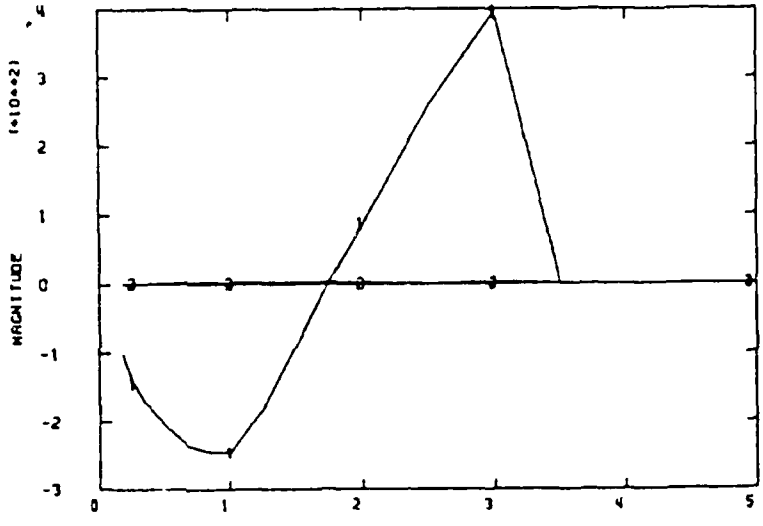

b. 3/4-in. plywood

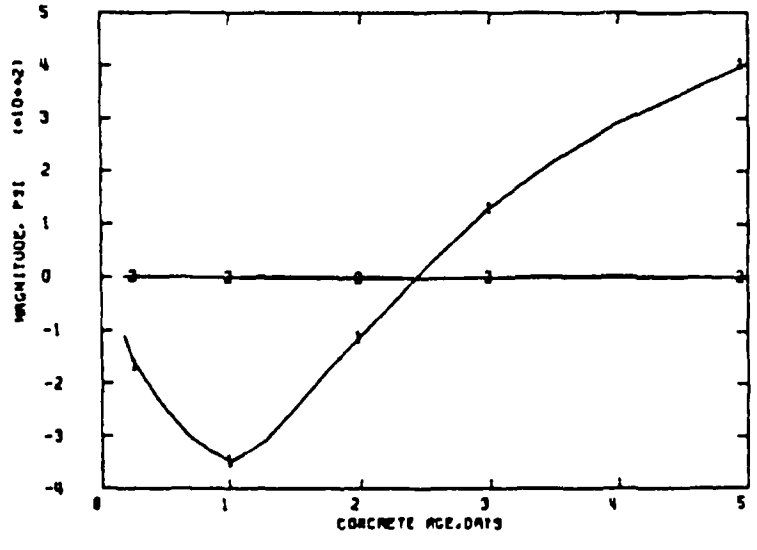

c. No heat transfer across boundary

Figure 30. Effects of form insulation on stress-time histories (stresses predicted at element 30)

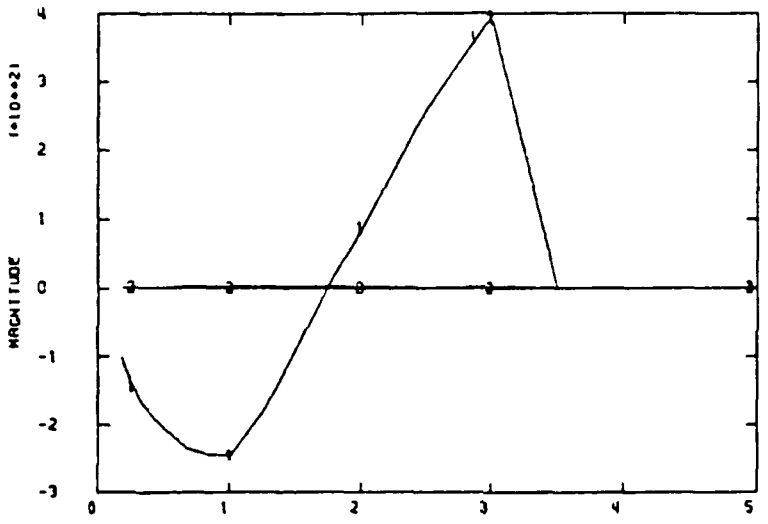

a. No bond breaker provided

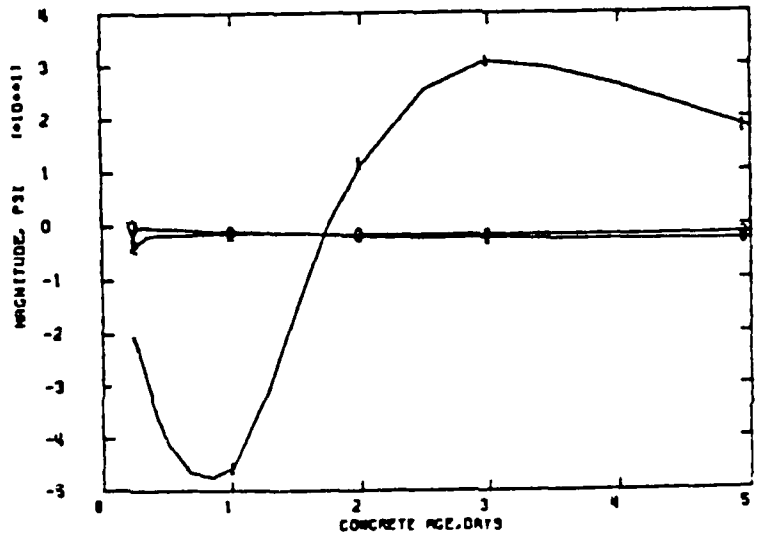

b. Bond breaker provided

Figure 31. Effects on bond breaker between old and new concrete on stress-time histories (stresses predicted at element 30)

occur. Possible solutions to the problem of providing a low-friction interface between the old and new concrete include placing a thin layer of sand or sheets of plastic prior to placing the new concrete. However, the structural impacts of using a bond breaker and the effects of dowels or anchors between the old and new concrete would have to be investigated.

Form Removal Time

24. Form removal time had a minimal effect on cracking within the resurfacing slab (Figure 32). Leaving the forms in place did prove beneficial up to 3 days after placement (Figure 32c).

Resurfacing Slab Thickness

25. Increasing the slab thickness over a range of 18 to 36 in. had a relatively significant effect on the stresses in the slab as can be seen in Figure 33. The magnitude and duration of compressive stresses are each increased. For the 36-in. slab, tensile cracking did not occur within the 5-day period of analysis, although once again cracking was imminent at that time. The significant increase in construction cost must be considered when evaluating the benefits of reduced cracking potentials in the thicker slab.

Dowel Bars

26. In all runs including dowel bars or reinforcing steel, the effect was to increase the rate of heat loss as heat was conducted through the dowels to the old concrete. Generally, this shortened the time before cracking as can be seen in Figure 34.

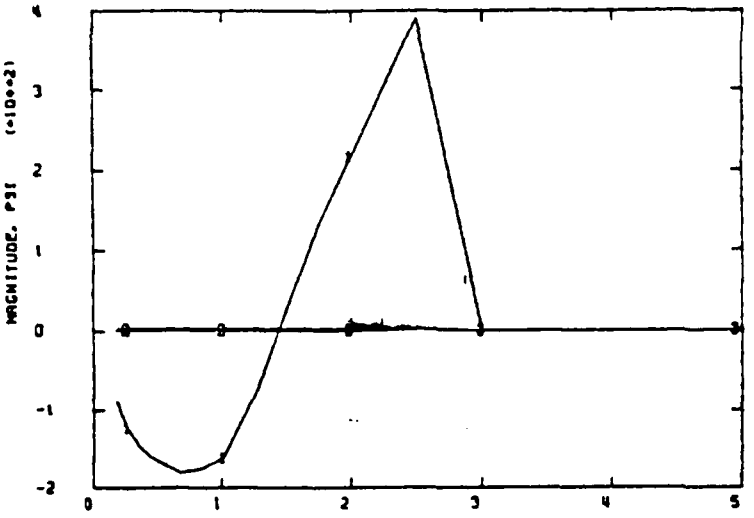

a. Forms removed instantly

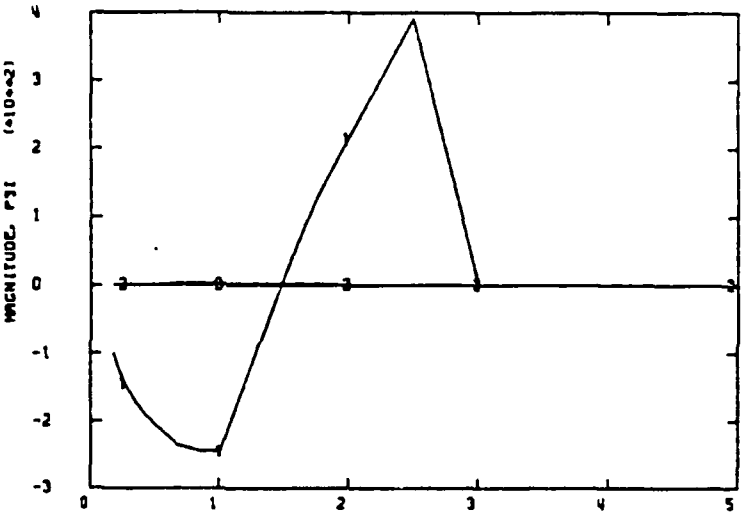

b. Forms removed at 1 day

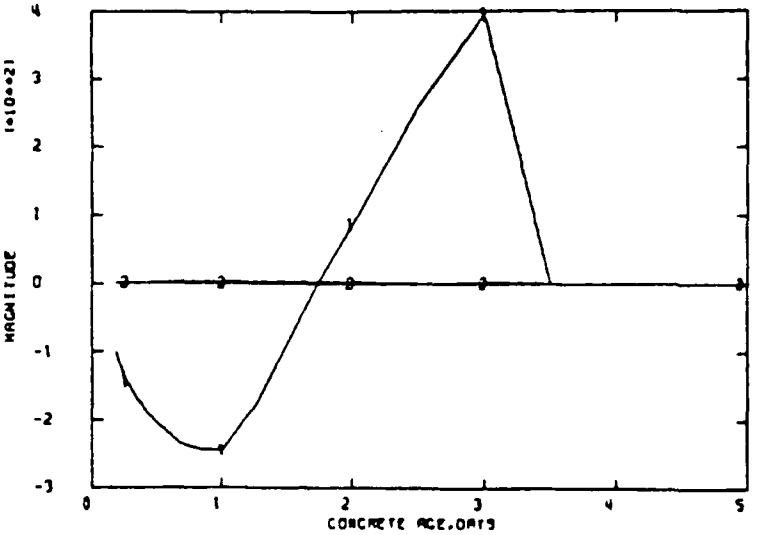

c. Forms removed at 5 days

Figure 32. Effects of form removal time on stress-time histories (stresses predicted at element 30)

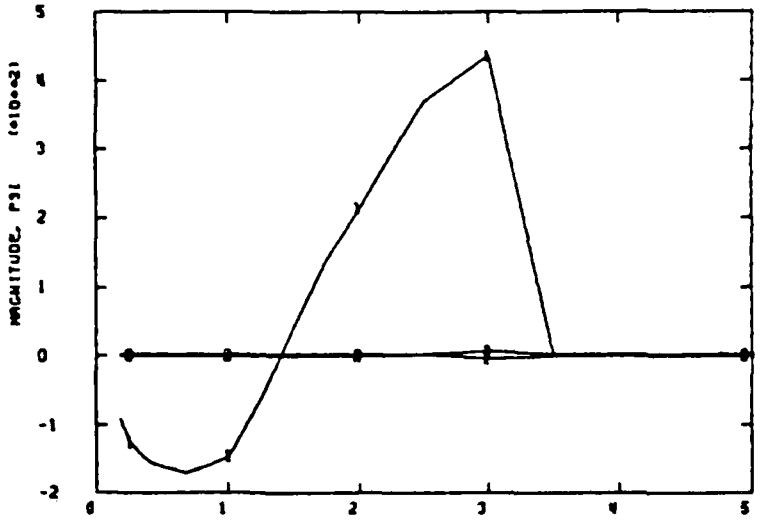

a. 12-in. slab

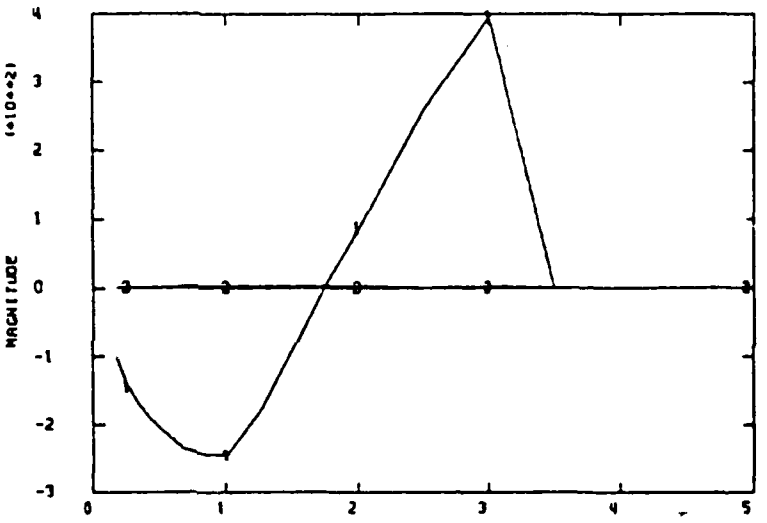

b. 18-in. slab

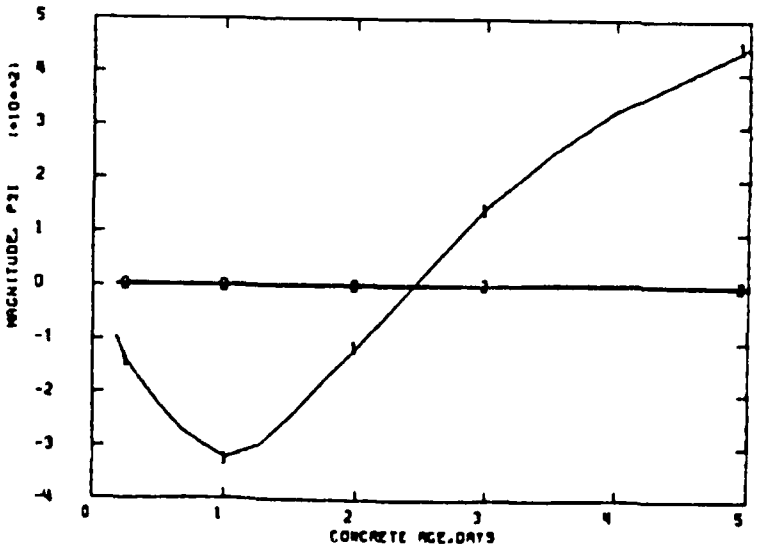

c. 36-in. slab

Figure 33. Effects of slab thickness on stress-time histories (stresses predicted at element 30)

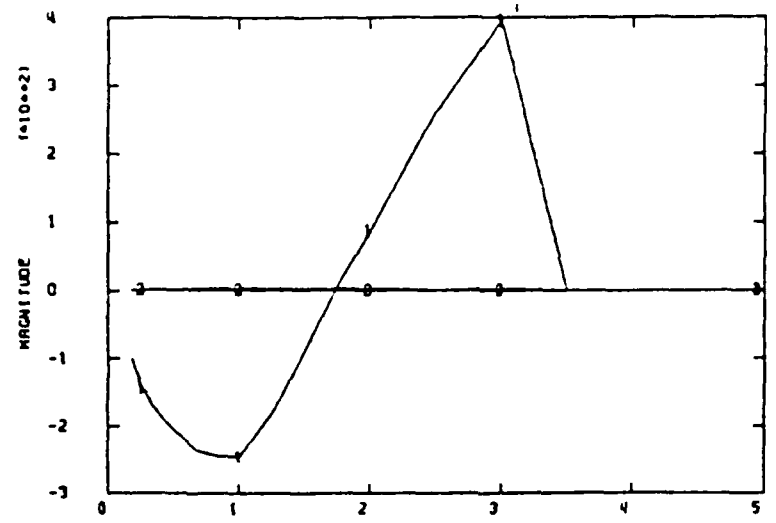

a. No dowels

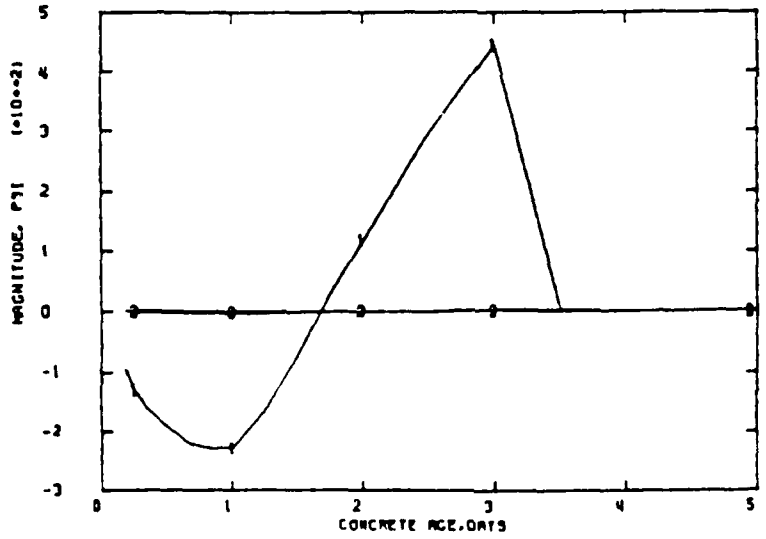

b. Dowels at 3 ft O.C.

Figure 34. Effects of dowels on stress-time histories (stresses predicted at element 30)

PART IV: CONCLUSIONS AND RECOMMENDATIONS

Conclusions

27. Lowering the placement temperature of the concrete overlay delayed but did not prevent cracking when shrinkage was included in the FE analyses.

28. Ambient temperatures can have a significant effect on cracking when these temperatures are at rather extreme values. With ambient temperatures very low (e.g., 25° F), cracks occur at the face of the resurfacing slab (Figure 28). Whereas when ambient temperatures are very high (e.g., 100° F), cracks occur along the interface of old and new concrete.

29. In essentially all of the analyses, shrinkage had a very significant effect on cracking. In every case, the effects of shrinkage were the same, the only difference being the time when the cracking occurred. This can be seen in Table 4.

30. Also, thickness of overlay slab has a significant effect on cracking, and for the 36-in. slab no cracking was observed within the analysis time period.

31. Cracking can be reduced or inhibited when a low-friction interface is developed between the old and new concrete.

Recommendations

32. Due to the dominant effect of shrinkage on the cracking problem, great care should be taken in curing overlay slabs. It is generally accepted that continuous moist curing is the curing method most likely to prevent cracking. Also, concrete mixture proportions which reduce or minimize autogenous shrinkage should be developed, evaluated, and used when possible.

33. Due to the fact that early-time material properties have a significant effect on predicted stresses and cracking, it is recommended that shrinkage, creep, moduli, etc. be carefully measured at a series of early times such as 1 day, 2 days, 3 days, etc. Additional test and complementary analysis programs should be developed and conducted to better define the effects of boundary conditions and overlay geometry.

34. The feasibility of using various types of low-friction interface materials or designs should be investigated especially for horizontal

overlays. Analyses and demonstration tests should be performed for an investigation of this type.